(NASA-CR-162994) RESEARCH IN PARTICLES AND FIELDS Semiannual Status Report, 1 Apr. 1979 - 31 Mar. 1980 (California Inst. of Tech.) 44 p HC A03/MF A01 CSCL 20H

N80-23110

Unclas
G3/72 18009

SPACE RADIATION LABORATORY (SRL)

CALIFORNIA INSTITUTE OF TECHNOLOGY

Pasadena, California 91105

SEMI-ANNUAL STATUS REPORT

for

NATIONAL AERONAUTICS AND SPACE ADMINISTRATION

Grant NGR 05-002-160*

"RESEARCH IN PARTICLES AND FIELDS"

for

1 April 1979 - 31 March 1980

Rochus E. Vogt, Principal Investigator
A. Buffington, Coinvestigator
L. Davis, Jr., Coinvestigator
E.C. Stone, Coinvestigator

* NASA Technical Officer: Dr. A.G. Opp, Physics and Astronomy Programs

TABLE OF CONTENTS

SEMI-ANNUAL STATUS REPORT

NASA Grant NGR 05-002-160

Space Radiation Laboratory (SRL)
California Institute of Technology

1 April 1979 - 31 March 1980

This report covers the research activities in Cosmic Rays and Theory of Particles and Fields in Space supported under NASA Grant NGR 05-002-160.

The report is divided into sections which describe the various activities, followed by a bibliography.

I. Cosmic Rays

This group's research program is directed toward the investigation of the astrophysical aspects of cosmic rays and γ rays and of the radiation environment of the Earth and other planets by means of energetic particle detector systems flown on spacecraft and balloons. The main efforts of the group, which are supported partially or fully by this grant, have been directed toward the following two categories of experiments.

A. EXPERIMENTS ON NASA SPACECRAFT

1. An Electron/Isotope Spectrometer (EIS) Launched on IMP-7 on 22 September 1972 and on IMP-8 on 26 October 1973

This experiment is designed to measure the energy spectra of electrons and positrons (0.16 to $\sim$ 6 MeV), and the differential energy spectra of the nuclear isotopes of hydrogen, helium, lithium, and beryllium ($\sim$ 2 to $\sim$ 50 MeV/nucleon). In addition, it provides measurements of the fluxes of the isotopes of carbon, nitrogen, and oxygen from $\sim$ 5 to $\sim$ 15 MeV/nucleon. The measurements from this experiment support studies of the origin, propagation, and solar modulation of galactic cosmic rays, the acceleration and propagation of solar flare particles, and the acceleration of charged particles in the Earth's magnetotail.

The data analysis activities continue to focus on correlative studies which are made possible for the first time by the comprehensive and extensive character of the IMP-7 and -8 data sets. The following talks and papers have resulted:

- o Simultaneous Two-Spacecraft Observations of the Magnetopause Electron Layer, (J.W. Bieber, and E.C. Stone, EOS Trans. AGU, 60, 909 1979).
- o Energetic Electron Bursts in the Magnetopause Electron Layer and in Interplanetary Space, (J.W. Bieber, E.C. Stone, Proceedings of Magnetospheric Boundary Layers Conference, Alpbach, Austria, p. 121, ESA SP-148, 1979).
- o Observations of 1-6 MeV Jovian Electrons at 1 AU and a Study of Their Propagation, (S.H. Hartman, Ph.D. Thesis, California Institute of Technology, 1979).
- o Characteristics of the Spectra of Protons and Alpha Particles in Recurrent Events at 1 AU, (R.A. Mewaldt et al., Geophys. Res. Ltrs. 6, 589, 1979).
- o Energetic Electron Bursts in the Magnetopause Electron Layer and Interplanetary Space, (J.W. Bieber, and E.C. Stone, EOS Trans. AGU, 60, 369, 1979).
- o Streaming Anisotropies of 1.2 - 2.3 MeV Protons and Their Interpretation, (E.C. Stone, EOS Trans. AGU, 60, 739, 1979).
- o Studies of Elemental and Isotopic Composition of Solar Flare Nuclei, (R.A. Mewaldt, Bull. Am. Phys. Soc. 24, 618, 1979).

Selected details of these studies are given below:

IMP Data Analysis:

During the past year, data from the Caltech instrumentation aboard IMP-7 and IMP-8 have been utilized in three major areas:

1) Energetic Upstream Electrons. Although sunward-streaming ions and low energy ($\lesssim$ 40 keV) electrons observed upstream of Earth's bow shock are commonly believed to be accelerated at the shock, our analysis shows that the high energy (> 200 keV) component of upstream electrons originates behind the shock and most probably has the same source as the permanent layer of energetic electrons adjacent to the magnetopause.

2) Simultaneous Two-Spacecraft Observations of the Magnetopause Electron Layer. The magnetopause electron layer tailward of Earth is an annular region encircling the magnetopause in which bursts of energetic electrons are almost continuously present. Whereas previous studies focused on determining the average global properties of the layer, the present investigation utilized two-spacecraft observations to study its microstructure. As a result of this study, it was possible to determine the approximate size of the source region for layer electrons and to distinguish between spatial and temporal variations within the layer.

3) Relationship of Open Field Lines in the Magnetotail to Geomagnetic Substorms. According to the neutral line theory of substorms, a substorm is triggered by the formation of an X-type neutral line in the near-Earth plasma sheet at which reconnection of magnetotail field lines occurs. According to this theory, a spacecraft located in the plasma sheet at $X \sim -30R_E$ would find itself on open field lines during at least a portion of the substorm expansive phase. Because a large streaming flux of energetic electrons indicates that the spacecraft is located on an open field line, we have examined the behavior of the AE index of geomagnetic activity and the behavior of the magnetotail field at times when intense energetic electron streaming is observed in the magnetotail. Preliminary results of this analysis strongly support the neutral line theory of substorms.

Details of the first two studies outlined above are given below. Because the third study is currently continuing, a detailed report will be deferred to a later time.

Energetic Upstream Electrons

Bursts of sunward-streaming energetic electrons are occasionally observed in interplanetary space upstream of the Earth's bow shock. Figure 1 presents IMP-8 data for an 8-hour period during which such bursts were observed. As shown in the lower left-hand corner, the spacecraft was located more than 10 R_E upstream of the dawn bow shock during this period. The bursty nature of upstream electrons is illustrated in the top panel, where intensity variations of a factor of 10 or more on a time scale of minutes are common. The next panel in Figure 1 illustrates the intense($\geq$ 50%) sunward streaming of these electrons. Finally, the angular distribution of electrons observed during the intense burst from 0705-0720 UT is shown in the lower right corner of Figure 1 along with the interplanetary field direction during this period. The streaming is seen to be field-aligned with virtually no particles in the backward (earthward-directed) hemisphere.

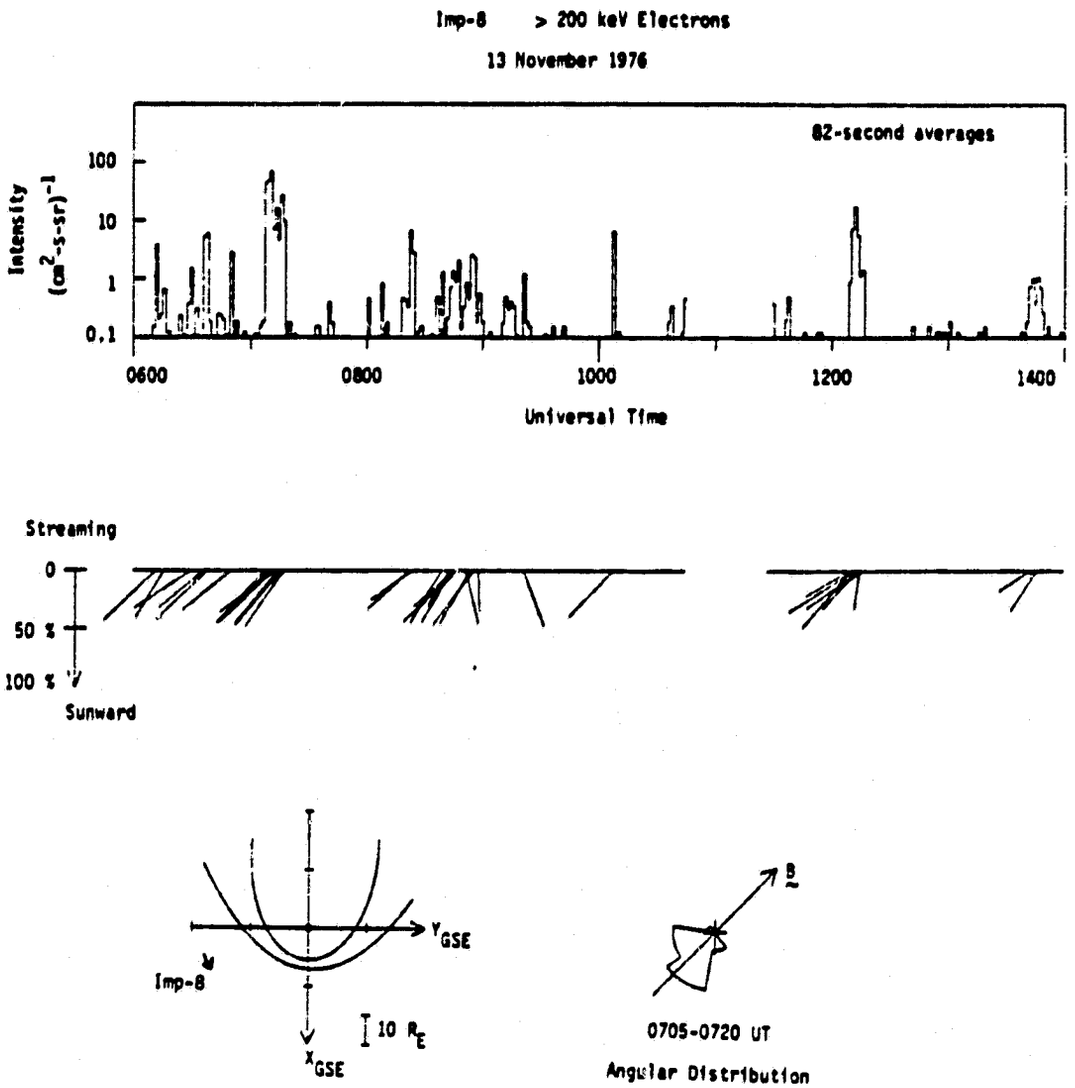

Figure 1

It has been found that a principal factor that determines whether or not a burst is observed is the favorability of the connection between Earth and the spacecraft along the interplanetary field line. To quantify this effect, a new coordinate system, called geocentric interplanetary medium (GIPM) coordinates, was defined. The GIPM coordinate system is essentially the GSE system rotated about the X_{GSE} axis in such a way that the Z-component of the interplanetary field vanishes in the new coordinate system. The magnetohydrodynamic calculations of Alksne show that the value of Z_{GIPM} is a direct measure of the degree of penetration of an interplanetary field line into the magnetosheath, with small values of Z_{GIPM} indicating the deepest penetration.

The dependence of upstream burst occurence on GIPM coordinates is illustrated in Figure 2 where the upper panel shows the trajectory of IMP-8 in the upstream region over a period of nearly 4 years, and the lower panel shows where bursts were observed during this same period. The trace of the IMP-8 trajectory is very irregular because the interplanetary field direction, which determines GIPM coordinates, can vary greatly on a time scale $\leq$ 1 hour. Figure 2 shows that although the spacecraft has fairly uniform access to a region within $\sim 30\ R_E$ of the $Z_{GIPM} = 0$ plane, the greatest number of bursts is observed dawnward of Earth near $Z_{GIPM} = 0$ on field lines that trace back into the inner

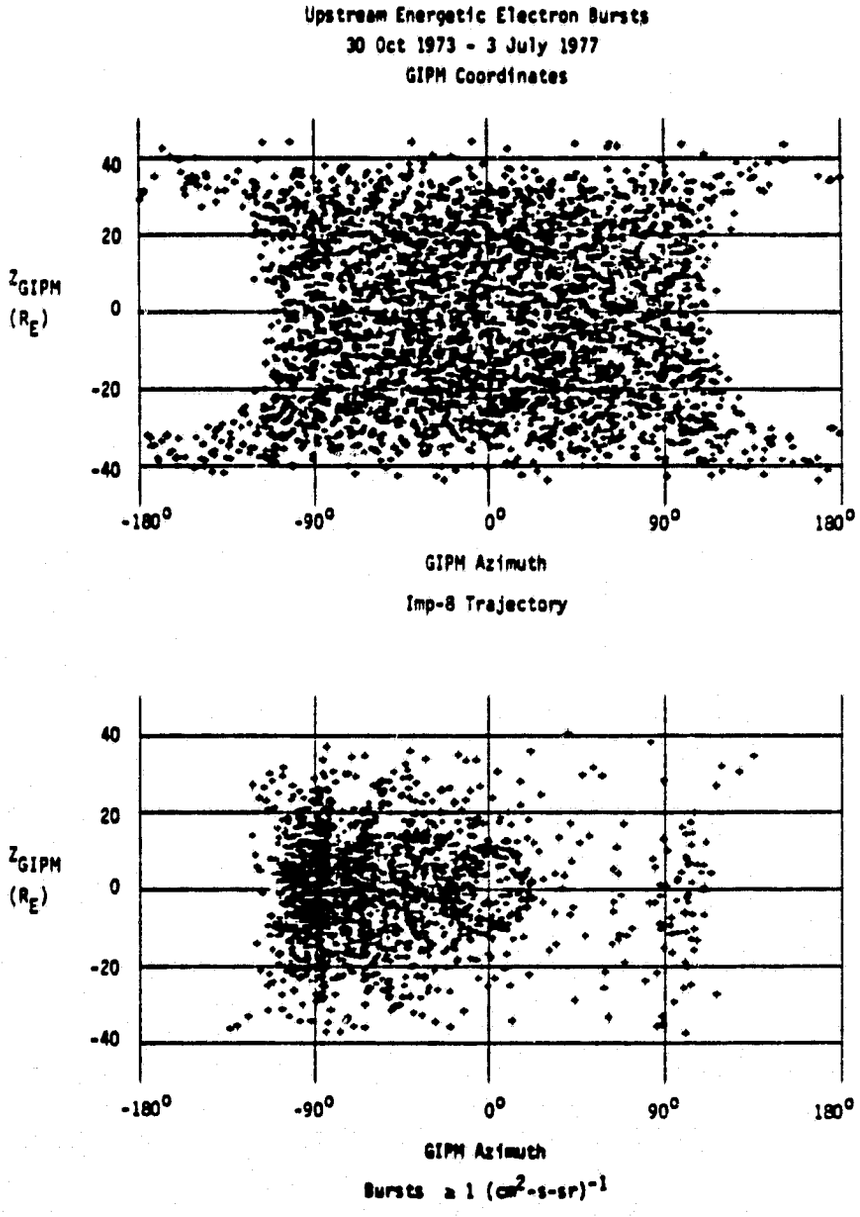

Figure 2

magnetosheath. From the data presented in Figure 2, the average total energy transported sunward by > 200 keV electrons was determined to be 2×10^{14} erg/s. This is comparable to the energy flow in the magnetopause electron layer reported by Baker and Stone. Thus it appears that the upstream electrons have the same source as the layer electrons, and that the upstream bursts are seen on the sunward extension of the field lines passing through the magnetopause electron layer. This interpretation is further supported by the similarity in the time scales of layer bursts and upstream bursts ($\sim$ 1-5 minutes) and by the similarity in the average energy spectral indices calculated for layer electrons and upstream electrons ($\gamma \sim 3.2$, where intensity $\propto E^{-\gamma}$).

Other investigators have concluded that ions and lower energy electrons ($\lesssim$ 40 keV) observed upstream of the bow shock are solar wind particles that have been accelerated at the shock. To determine whether the > 200 keV upstream electrons might also originate at the shock, a statistical study of energetic electrons in the vicinity of the dawn shock was conducted. Figure 3 depicts average angular distributions and streaming vectors at 3-hour intervals from 12 hours before till 12 hours after the shock crossing. Although anisotropies in the magnetosheath are small, the streaming of 3.1 $\pm$ 0.1 % observed just before crossing the shock is significant and is clearly directed towards the shock. This fact is inconsistent with a shock source for the > 200 keV electrons. After crossing the shock into the upstream region, the average streaming magnitude increases by a factor of $\sim$ 10 and the average intensity decreases by about the same factor, but the component of the net streaming flux along the shock normal remains nearly constant as the shock is crossed. Thus the observed flow of the electrons towards the shock in the magnetosheath is almost exactly what is required to supply the observed upstream sunward flow.

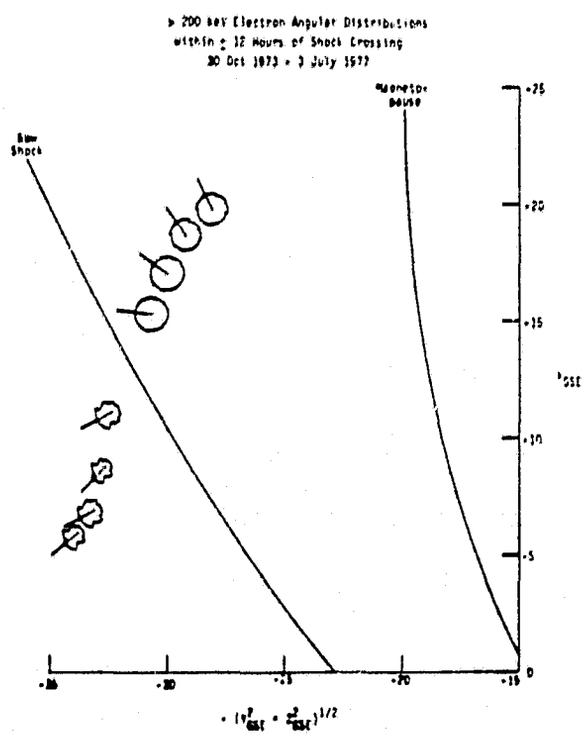

Figure 3

Finally, it is possible to deduce the mean free path of > 200 keV electrons

in the magnetosheath by applying the leaky box model of particle propagation, which was originally developed for galactic cosmic rays, to the data of Figure 3. The nearly isotropic angular distributions seen in the magnetosheath suggest that energetic electrons are confined by scattering in the magnetosheath and escape only when they cross the shock into the upstream region, where scattering is less effective, as evidenced by the large streaming anisotropies seen upstream.

According to the leaky box model, the mean free path λ is related to the streaming magnitude S and scale length L of the confinement region by $\lambda = 3SL$. Taking $L \sim 10\ R_E$, this implies a mean free path of $\lambda \sim 1\ R_E$ for > 200 keV electrons in the magnetosheath. This value is consistent with the mean free path calculated by applying quasilinear pitch angle scattering theory to observed magnetosheath magnetic power spectra.

Simultaneous Two-Spacecraft Observations of the Magnetopause Electron Layer

During the entire period of IMP data coverage, 11 time intervals were found during which IMP-7 and IMP-8 were simultaneously in the magnetopause electron layer. One such interval is depicted in Figure 4. The top panel shows the > 200 keV electron flux observed on IMP-7 and IMP-8. The bars above the flux profiles indicate the location of the spacecraft, whether in the magnetosphere (MSP), boundary layer (BL), or magnetosheath (MSH). Hourly averages of the angular distributions observed on the two spacecraft are shown below the flux plots. Although the fluxes observed on IMP-7 and IMP-8 were clearly correlated throughout the 8-hour interval shown in Figure 4, the period of particular interest for this study is from 1910-2037 UT, when both spacecraft were

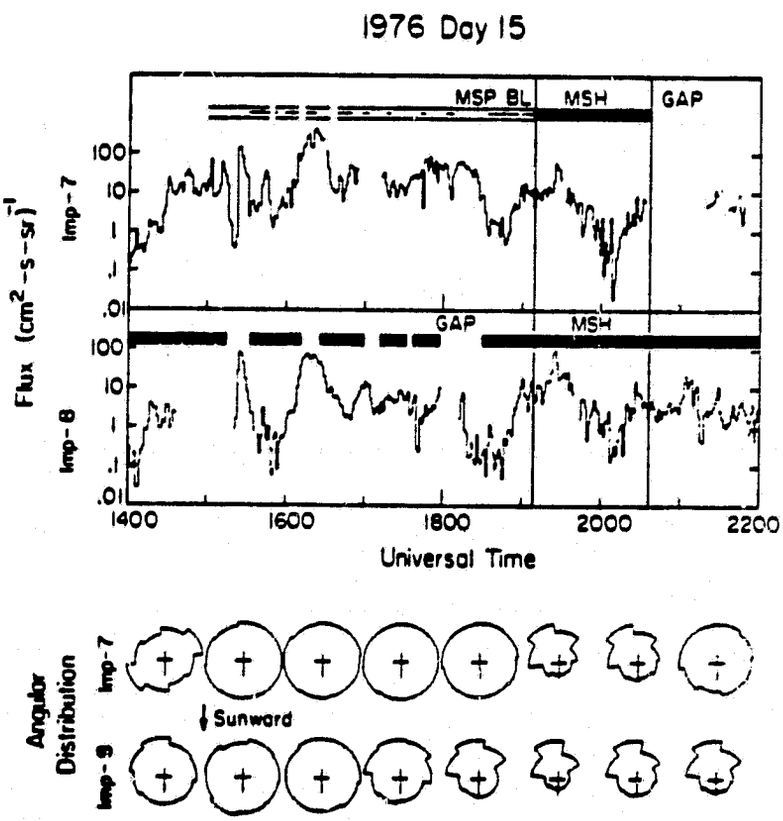

Figure 4

located in the magnetosheath and were observing the intense tailward streaming that is characteristic of the magnetopause electron layer.

Figure 5 presents a scatter plot of the flux observed at IMP-8 (82-second averages) versus the simultaneously observed flux at IMP-7 for the 1910 - 2037 UT period. The points clearly tend to lie along the line of equal fluxes. The cross-correlation coefficient calculated for this simultaneous crossing, during which the average separation of the two spacecraft was 12.6 R_E, was $R_{cross} = 0.78$.

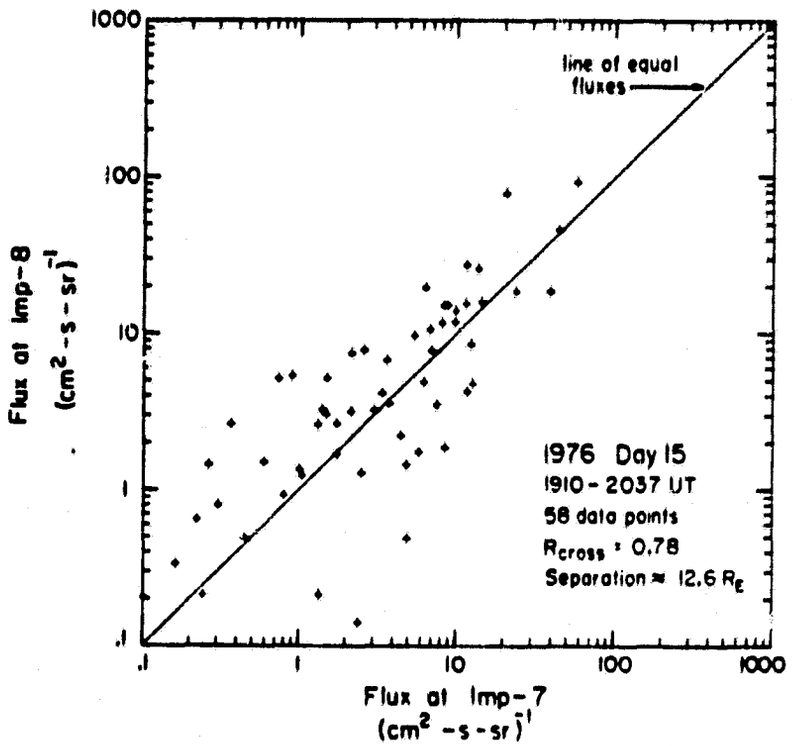

Figure 5

Cross-correlation coefficients for each of the 11 simultaneous crossings in this study are plotted in Figure 6 as a function of the average spacecraft separation during the crossing. None of the four crossings with separations > 40 R_E, for which the spacecraft were located on opposite sides of the magnetotail, showed a significant degree of correlation. Of the remaining seven simultaneous crossings, for which the spacecraft were located on the same side of the magnetotail, two showed no significant correlation in electron flux, two showed a moderate degree of correlation ($R_{cross} \sim 0.5$), and three were highly correlated ($R_{cross} \geq 0.7$). From this it can be concluded that electron fluxes in the

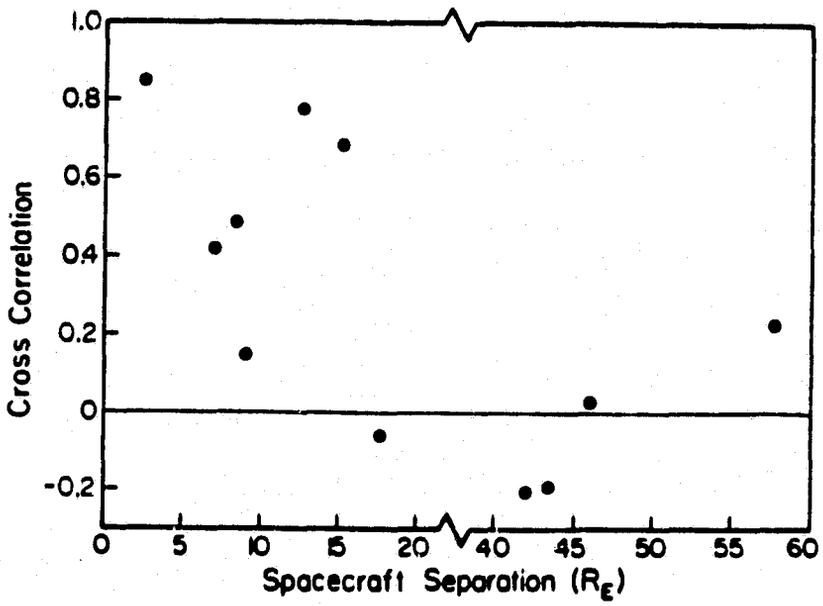

Figure 6

magnetopause electron layer are often temporally correlated over distance scales $\lesssim 20\ R_E$, but are uncorrelated over larger distances. This $20\ R_E$ distance scale may be interpreted as a direct measure of the size of the source region of layer electrons. If the source were much smaller, then to explain the observed correlation length scales, the electrons would have to propagate $\sim 20\ R_E$ across magnetic field lines while travelling from the source to the observation point at $X_{GSM} \sim -30\ R_E$. In view of the large field-aligned anisotropies seen in the layer, such rapid cross-field transport seems unlikely.

Additional information about the microstructure of the layer can be obtained from the autocorrelation function of electron fluxes. This is calculated by comparing the flux at a given spacecraft at some time t with the flux observed at the same spacecraft at a later time $t + \delta t$. As δt increases, the calculated autocorrelation coefficient decreases, and the rate of decrease provides a quantitative measure of the time scale for flux variations. For the layer crossings treated in this study, this burst time scale was typically in the range 1-5 minutes.

By comparing the cross-correlation coefficient with the autocorrelation function, it is possible to determine whether the temporal flux variations seen in the layer reflect an intrinsic variation of the source, or whether they reflect the convection of spatial variations past the spacecraft. For a simultaneous crossing, the degree of correlation of electron flux over a distance scale $< r >$, where $< r >$ is the average spacecraft separation, is known. In a time $\delta t = < r >/V$, where V is plasma flow velocity, an element of plasma that was previously located a distance $< r >$ upstream will be convected to each spacecraft. If the source does not vary significantly during the time δt, then the value of the autocorrelation coefficient for a delay time $\delta t = < r >/V$ should be comparable to the measured cross-correlation coefficient. On the other hand, if the source does vary significantly during the time δt, the autocorrelation coefficient will be reduced relative to the cross-correlation coefficient.

The comparison of correlation coefficients described above has been carried out for each of 11 crossings in this study. The results are presented in Figure 7, where the autocorrelation coefficient is plotted as a function of the cross-correlation coefficient. Because the autocorrelation function can be determined separately for each spacecraft, two values of the autocorrelation coefficient are available for each crossing. These two values are connected

by vertical lines in Figure 7. In most cases, the two independently calculated values agree fairly well. Most of the points in Figure 7 lie near the diagonal line, where the autocorrelation and cross-correlation coefficients are equal. This indicates that temporal variations in the magnetopause electron layer can be explained almost entirely in terms of convection. As explained above, if the source did vary significantly during the convection time, then the autocorrelation coefficient would be less than the cross-correlation coefficient, and the points in Figure 7 would lie consistently below the diagonal line. Because this is clearly not the case in Figure 7, it can be concluded that the source varies on a time scale longer than the typical convection times of 1-3 minutes.

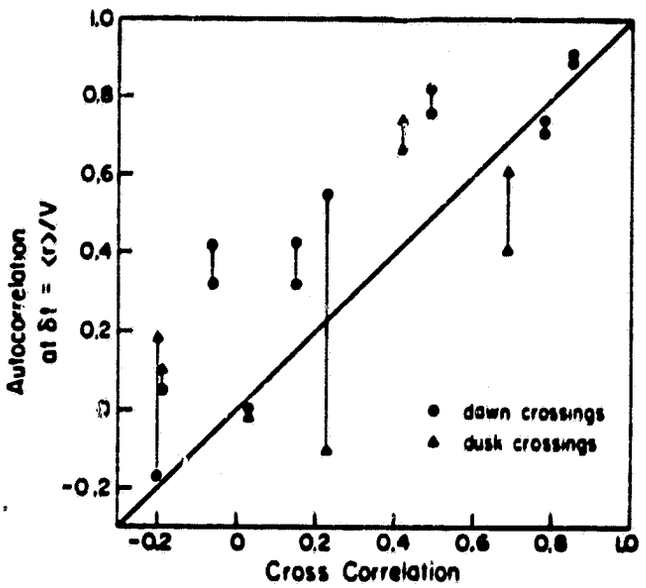

Figure 7

In summary, the study of simultaneous layer crossings has demonstrated that:

1) the source region for layer electrons is $\sim 10 - 20\ R_E$ in size;
2) time variations of energetic electron flux are caused by the convection of spatial variations past the spacecraft rather than by an intrinsic variation of the source;
3) The source must vary on a time scale longer than ~ 3 minutes.

The implications of these conclusions for the source and acceleration mechanism of layer electrons are currently under investigation.

2. <u>An Interstellar Cosmic Ray and Planetary Magnetospheres Experiment on the Voyager 1 & 2 Missions Launched in 1977</u>

This experiment is conducted by this group (SRL) in collaboration with F.B. McDonald, A.W. Schardt and J.H. Trainor (Goddard Space Flight Center), W.R. Webber (University of New Hampshire), and J.R. Jokipii (University of Arizona), and has been designated the Cosmic Ray Subsystem (CRS) for the Voyager Missions. The experiment is designed to measure the energy spectra, elemental and isotopic composition, and streaming patterns of galactic

cosmic-ray nuclei from H to Fe over an energy range of 0.5 to 500 MeV/nucleon and the energy spectra of electrons with 3-100 MeV. These measurements will be of particular importance to studies of stellar nucleosynthesis, and of the origin, acceleration, and interstellar propagation of cosmic rays. Measurements of the energy spectra and composition of energetic particles trapped in the magnetospheres of Jupiter and Saturn will be used to study their origin and relationship to other physical phenomena and parameters of these planets. Measurements of the intensity and directional characteristics of solar and galactic energetic particles as a function of heliocentric distance will be used for in situ studies of the interplanetary medium and its boundary with the interstellar medium.

The CRS flight units on both Voyager spacecraft have been operating successfully since the Voyager launches in August and September 1977. The CRS team participated in the Voyager 1 and 2 Jupiter encounter operations in March and July 1979, respectively.

The basic data processing system and software are in routine operation. The processing and scientific analysis of Voyager data rely heavily on the grant supported multi-user, interactive data analysis facility, which continues to be evolved towards greater efficiency and usefulness. Experience with the system has shown that both the quantity and quality of science results from a given set of observational data is closely related to the flexibility, sophistication, and accessibility of the SRL small-computer data analysis system.

The Voyager data existing so far already represent an immense and diverse data base, and a number of scientific problems are under analysis. These investigation topics range from the study of galactic particles to particle acceleration phenomena in the interplanetary medium, to plasma/field energetic particle interactions, to acceleration processes on the sun, to studies of elemental abundances of solar, planetary, interplanetary, and galactic energetic particles.

The following publications and papers for scientific meetings, based on Voyager data, were generated:

- Voyager 1: Energetic Ions and Electrons in the Jovian Magnetosphere (R.E. Vogt et al., Science, 204 , 1003, 1979).

- The Voyager 1 Encounter with the Jovian System (E.C. Stone and A.L. Lane, Science, 204, 945, 1979).
- Elemental Composition ($1 \leq Z \leq 28$) of Solar Energetic Particles in 1977 and 1978 (W.R. Cook et al., 16th Intl. Cosmic Ray Conference Papers, 12, 265, 1979).
- Voyager 2: Energetic Ions and Electrons in the Jovian Magnetosphere (R.E. Vogt et al., Science, 206, 984, 1979).
- Voyager 2 Encounter with the Jovian System (E.C. Stone and A.L. Lane, Science, 206, 925, 1979).
- Spacecraft Measurement of the Elemental and Isotopic Composition of Solar Energetic Particles (R.A. Mewaldt, Submitted to Proc. of Conf. on Ancient Sun, Lunar and Plan. Science Institute, Houston, 1980).
- Elemental Composition of Solar Energetic Nuclei (W.R. Cook, E.C. Stone and R. Vogt, accepted for publication, Ap. J. Letters, 1980).
- The Elemental Composition and Anisotropies of Low Energy Cosmic Rays Using Voyager Data (E.C. Stone et al., Bull. Am. Phys. Soc. 24, 564, 1979).
- Studies of Elemental and Isotopic Composition of Solar Flare Nuclei (R.A. Mewaldt, Bull. Am. Phys. Soc. 24, 618, 1979).
- The Charge and Energy Spectra of Low Energy Galactic Cosmic Rays (F.B. McDonald et al., Bull. Am. Phys. Soc. 24, 564, 1979).
- The Modulation and Radial Variation of the Anomalous Helium and Oxygen Components Observed by Voyagers 1 and 2 (N. Lal et al., Bull. Am. Phys., 24, 564, 1979).
- The Effect of Coronal Transport on Energetic Solar Particles (T.F. Conlon et al., Bull. Amer. Phys. Soc. 24, 659, 1979).
- Source Variations of Interplanetary Jovian Electrons: Voyagers 1 and 2 (T.F. Conlon et al., EOS Trans. AGU, 60 354, 1979).
- An Overview of the Voyager 1 Encounter with Jupiter (E.C. Stone, EOS Trans. AGU, 60, 304, 1979).
- High Energy Particles (R.E. Vogt et al., EOS Trans. AGU, 60, 305, 1979).
- Energetic Sulfur and Oxygen Nuclei in the Jovian Magnetosphere (N.E. Gehrels et al., EOS Trans. AGU, 60, 919, 1979).
- Voyager Mission Overview (Stone, Bull. Amer. Astron. Soc. 11, 583, 1979).
- The Detection of Interplanetary Protons Deep in Jupiter's Magnetosphere (T.F. Conlon et al., EOS Trans. AGU, 60, 919, 1979).

Further details of two of these studies are given as follows:

Elemental Composition of Solar Energetic Nuclei

First results from the investigations of the elemental composition of solar energetic nuclei with the Low Energy Telescope (LET) system of this group's cosmic-ray instruments on the Voyager 1 & 2 spacecraft were discussed in the April 1978 - 31 March 1979 status report. Analysis of these very exciting data has been continued as part of a doctoral dissertation of W.R. Cook, and a paper: "Elemental Composition of Solar Energetic Nuclei" has been accepted for publication by Ap. J. Letters. Figure 8 summarizes a representative set of solar abundance data (relative to silicon). "SEP" are the solar energetic nuclei abundances (8 - 15 MeV/nuc) from four solar energetic particle events in the September 1977 through May 1978 period. These four events were selected for

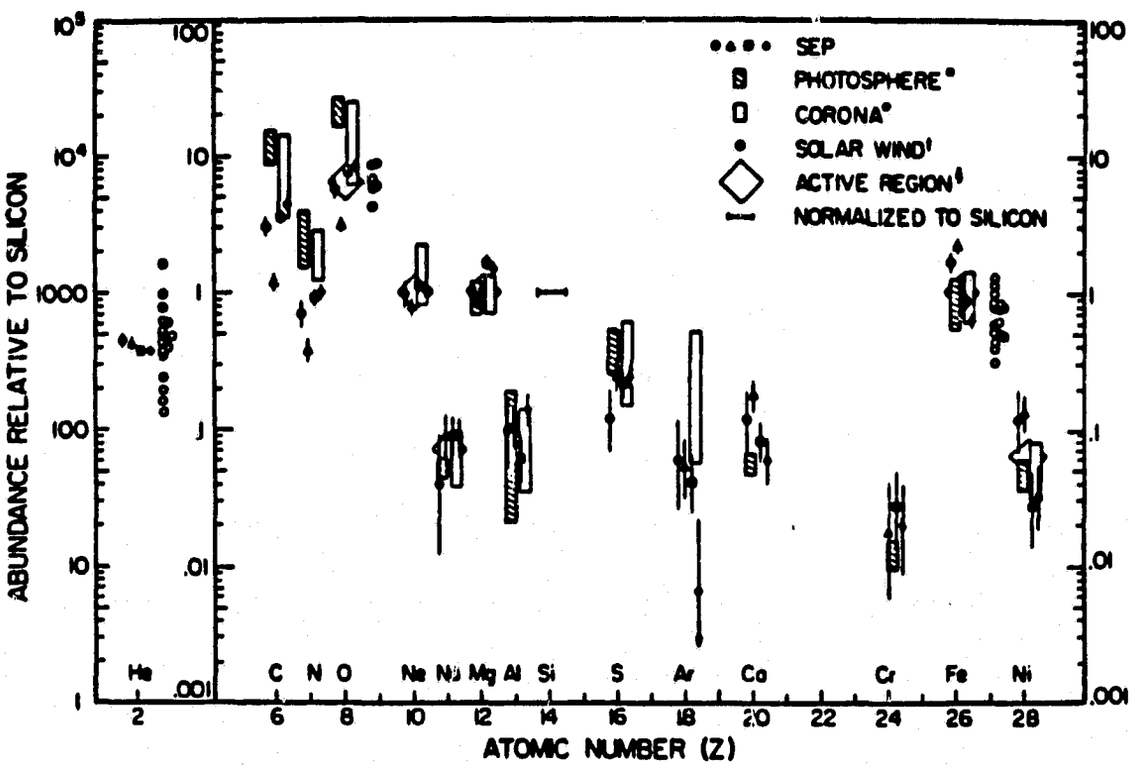

Figure 8

in-depth analysis because of the apparent energy independence of their abundance ratios with the expectation that the possible effects of acceleration and propagation biases may be small. Shown for comparison, are abundances derived from data

compilations on the photosphere and the corona, the solar wind, and an active coronal region. Although the SEP composition varies from flare to flare, the average SEP abundances are similar to those of other sources for all elements shown except carbon, nitrogen, and oxygen where the SEP values are persistently low relative to those of the photosphere, as is oxygen in the solar wind and in active region measurements.

Figure 9 illustrates the systematics of the SEP flare to flare composition variations by comparing the SEP elemental composition of the four selected events, $A_{Z,i}$, to the 4-event average A^*_Z. In each of the four events (a-d) the deviations of the SEP abundances from the average may be considered monotonic functions of nuclear charge Z in the range $6 \leq Z \leq 28$. In particular, the flare to flare abundance variations of C,N,O are correlated, as are the abundance variations of Ca, Fe, and Ni. The abundance variations of C, N, and O are anticorrelated with those of Ca, Fe, and Ni relative to Si. The Z - ordering of the abundance variations is not followed by He, whose abundance relative to Si is approximately the same for all four events. The correlations seen in Figure 9 suggest that the SEP elemental composition may be described by an average composition and a systematic deviation which varies in strength, but not in character, from event to event. In particular, the so-called "Fe-rich" events do not stand out as a separate class of events.

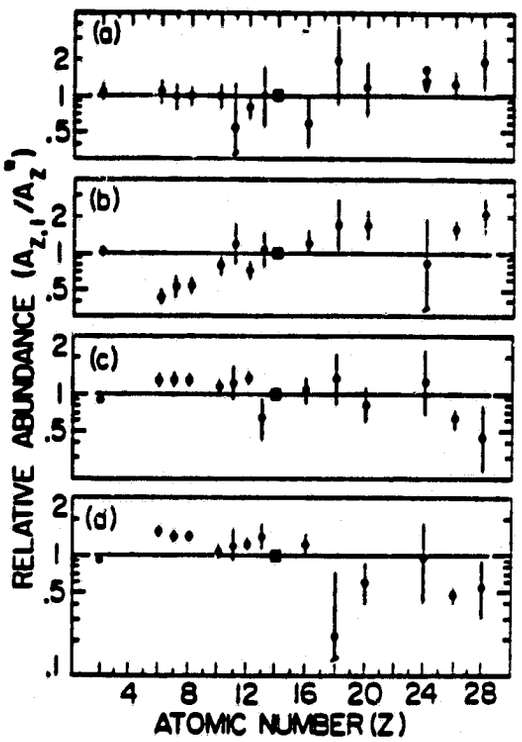

Figure 9

Figure 10 shows a comparison (ratios) of the 4-event average SEP abundances with those obtained for the photosphere, the corona, the solar wind (SW), and the galactic cosmic ray source (GCRS). Figure 10a illustrates that relative to the photosphere, the average SEP abundances of C, N, and O, and to a lesser extent, S,

are depleted with respect to the higher Z elements ($11 \leq Z \leq 28$). The comparison of coronal abundances (a mixed-origin compilation) to the average SEP composition (Figure 10b) shows a relative depletion of SEP C, N, and O which is less pronounced than that for the photosphere. The large error bars result mostly from the spread of coronal abundance measurements. Several recent coronal measurements (open symbols of Figure 3b) show good agreement with the average SEP composition, even for elements like N and O. Figure 10c shows that the solar wind and the average SEP abundances are in good agreement.

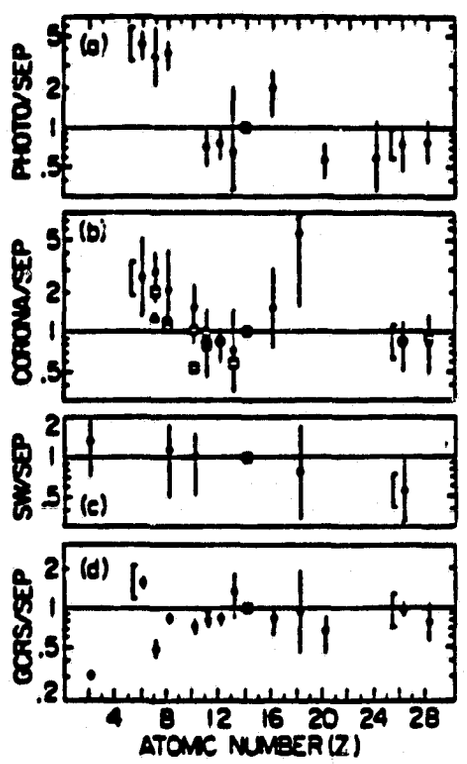

Figure 10

The overall similarity of the average SEP elemental composition and that measured for the solar wind and corona and in particular the evidence for a common depletion of oxygen relative to the photosphere, suggest that the differences in the average SEP and photosphere elemental composition may be related to basic plasma processes occurring on the sun, and that the SEP data may represent a powerful new tool to directly study coronal abundances.

Figure 10d compares our average SEP elemental composition and that of the galactic cosmic ray source (GCRS). SEP and GCRS abundances are similar for elements oxygen through nickel, but significant differences occur for He, C, and N. These comparisons are important to considerations of whether flaring stars may introduce the GCR source material into a galactic accelerator, in which case the GCRS elemental composition will not be considered a clear signature of recent nuclear processing in pre-supernovae or in supervonae explosions.

Energetic Oxygen and Sulfur Ions in the Jovian Magnetosphere

The Low Energy Telescopes (LETs) of the Cosmic Ray Subsystem (CRS) on Voyagers 1 and 2 provided an important tool for studying energetic ion population in situ

during the encounters with the Jovian magnetosphere. The LETs measured the energy spectrum, elemental composition, and flow patterns of energetic heavy nuclei ($7 < E < 14$ MeV/nuc).

Both the Voyager 1 and 2 passages into the Jovian magnetosphere revealed distinctly different energetic heavy ion populations in the inner and outer regions of the magnetosphere. This discovery is illustrated in Figure 11, showing the element (Z = nuclear charge) distributions measured by the Voyager 1 LET system (a) within ~ 5.8 R_j (Jupiter radii), and (b) outside 11 R_j. The outer region (≥ 11 R_j) of the magnetosphere was populated by energetic heavy ions of essentially "solar system" - like elemental composition, while the inner region (≤ 5.8 R_J) was dominated by enhanced fluxes of oxygen, sulfur (and sodium) ions with respect to carbon and nitrogen. The inner region composition appears similar to that of the Io Torus plasma, indicating a possible common origin in the volcanic ejecta of Io. However, the plasma and the energetic nuclei must undergo quite different processes subsequently since the injection energies ($\sim 5 \times 10^{-3}$ eV/nuc $\rightarrow$ 1 km/sec) and the plasma corotation energies (~ 15 eV/nuc) are much lower than the heavy ion energies (~ 10 MeV/nuc). In order to determine the magnetospheric domain where the post-acceleration of the heavy ions may take place, it is important to determine the radial distribution and flow patterns of the energetic heavy ions. Figure 12 shows the differential energy spectra of oxygen ions at radial distances of ~ 10 R_J and ~ 12 R_J respectively. The dashed line indicates the predicted energy spectrum at 10 R_J if the oxygen nuclei observed at 12 R_J were related to those at 10 R_J by lossless diffusion, under conservation of phase space density $J_\perp / B$. In fact, we observe the phase space density to decrease between 12 R_J and 10 R_J by about a factor of 10. The positive radial gradient of $\frac{J_\perp}{B}$ is a direct indication that

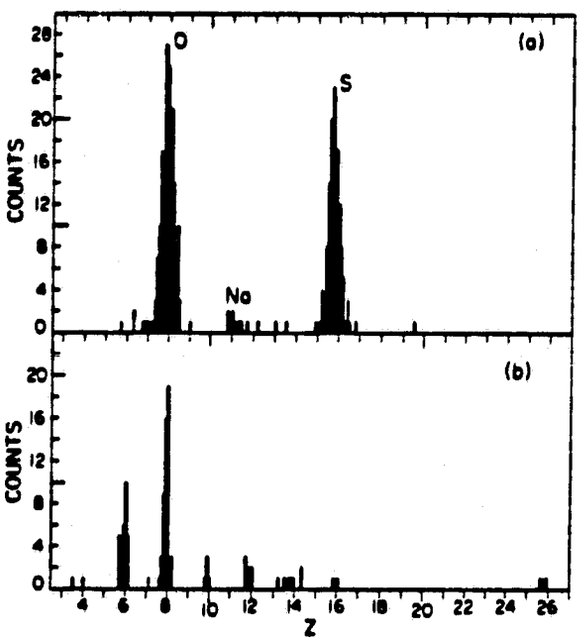

Figure 11

the enhanced energetic oxygen fluxes in the inner region of the Jovian magnetosphere are diffusing inward (while experiencing losses in intensity). This result appears to rule out an acceleration site for the energetic heavy oxygen ions near the Io orbit. It is more likely that these particles undergo charge exchange (as proposed by Eviator, Mekler and Coroniti for Na) near Io's orbit after having reached corotation velocities, escape as neutrals to the outer magnetosphere, became re-ionized, and then are accelerated in their process of inward diffusion.

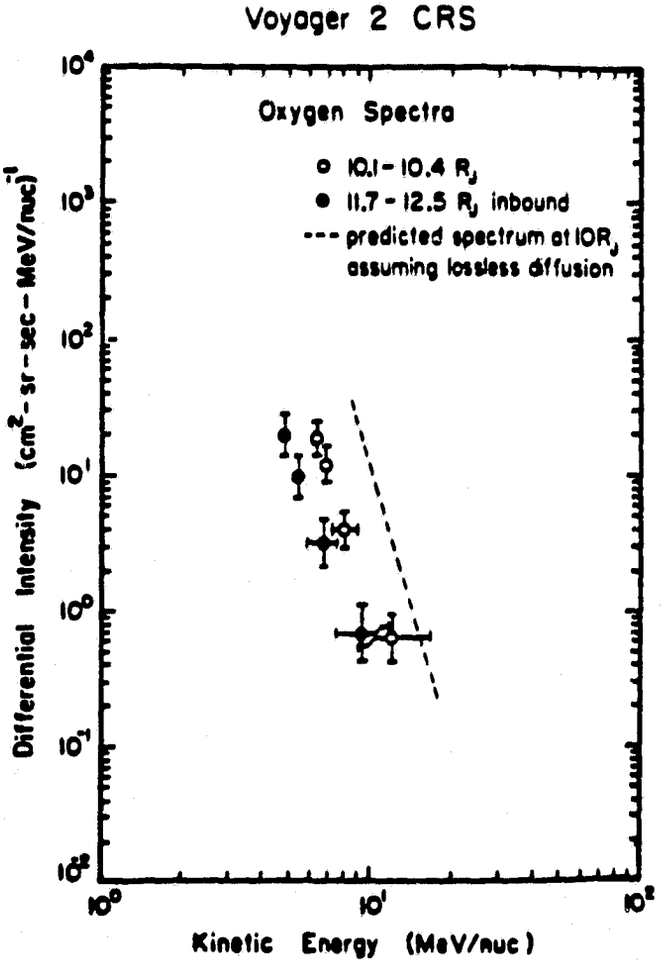

Figure 12

3. A Heavy Isotope Spectrometer Telescope (HIST) Launched on ISEE-3 in August 1978

HIST is designed to measure the isotopic abundances and energy spectra of solar and galactic cosmic rays for all elements from lithium to nickel ($3 \leq Z \leq 28$) over an energy range from several MeV/nucleon to several hundred MeV/nucleon. Such measurements are of importance to the study of the isotopic constitution of solar matter and of cosmic ray sources, the study of nucleosynthesis, questions of solar-system origin, studies of acceleration processes and studies of the life history of cosmic rays in the galaxy.

HIST was successfully launched on ISEE-3 and provided high resolution measurements of solar and galactic cosmic ray isotopes until December 1978. Since that time, the instrument has been operating as an element spectrometer for solar flare studies.

The continuing analysis of the isotopic data has resulted in the following talks and papers:

- Spacecraft Measurements of the Elemental and Isotopic Composition of Solar Energetic Particles, (R.A. Mewaldt, Conference on the Ancient Sun, Boulder, Colorado, 1979).
- Satellite Measurements of the Isotopic Composition of Galatic Cosmic Rays, (R.A. Mewaldt et al., 16th International Cosmic Ray Conf., Kyoto, Japan, Conf. Papers 12, 86, 1979).
- High-Resolution Measurements of Galactic Cosmic-Ray Neon, Magnesium, and Silicon Isotopes, (R.A. Mewaldt, et al., Ap. J. Letters 235, L95, 1980).
- The Isotopic Composition of Solar Flare Accelerated Neon, (R.A. Mewaldt et al., Ap. J. Letters 231, L97, 1979).
- The Isotopic Composition of Heavy Nuclei Accelerated in Solar Flares, (J.D. Spalding et al., EOS Trans. AGU, 60, 907, 1979).
- Isotopic Measurements of Solar and Galactic Cosmic Rays, (R.A. Mewaldt, EOS Trans. AGU, 60, 907, 1979).
- The Isotopic Composition of Energetic Solar Flare Nuclei from Carbon Through Iron, (R.A. Mewaldt et al., 16th International Cosmic Ray Conf., Kyoto, Japan, Conf. Papers 5, 74, 1979).
- Studies of Elemental and Isotopic Composition of Solar Flare Nuclei, (R.A. Mewaldt, Bull. Am. Phys. Soc. 24, 618, 1979).
- Satellite Measurements of the Isotopic Composition of Galactic Cosmic Rays, (J.D. Spalding et al., Bull. Am. Phys. Soc. 24, 692, 1979).
- Isotopic Measurements of Energetic Heavy Nuclei in the Solar Flares (R.A. Mewaldt et al., Bull. Am. Phys. Soc. 24, 694, 1979).

The first high resolution measurements of galactic cosmic ray Ne, Mg, Si, and Fe are described as follows:

High Resolution Measurements of Galactic Cosmic Ray Neon, Magnesium, and Silicon Isotopes

Our present understanding of the synthesis of the elements is based mainly on the comparison of the predictions of detailed theoretical models with the

observed distribution of isotopes in primitive solar system matter such as meteorites. Galactic cosmic ray nuclei provide a sample of matter from outside the solar system, which, in view of its younger age and possible association with supernovae, may have experienced a different nucleosynthetic history. Because the elements neon, magnesium, and silicon each possess more than one relatively abundant isotope and because they are the result of several nucleosynthetic processes, they are excellent choices for investigating possible isotopic differences between the galactic cosmic ray source and the solar system.

The individual isotopes of galactic cosmic ray Ne, Mg, and Si have been clearly resolved for the first time using data from the Caltech Heavy Isotope Spectrometer (HIST) on ISEE-3. Our results suggest that the cosmic ray source is enriched in ^{22}Ne, ^{25}Mg, and ^{26}Mg when compared to the solar system. In particular, we find $(^{25}Mg + {}^{26}Mg)/{}^{24}Mg = 0.49\ ^{+.23}_{-.14}$ compared to the solar system value of 0.27, suggesting that the cosmic ray source and solar system material were synthesized under different conditions.

HIST is designed to measure the isotopic composition of solar, galactic, and interplanetary cosmic ray nuclei for the elements Li to Ni in the energy range from ~5 to ~250 MeV/nucleon. The HIST telescope, shown schematically in Figure 13 consists of an array of solid state detectors, including a pair of two-dimensional position-sensitive detectors which determine individual particle trajectories, thereby leading to significant improvement in isotope resolution over previous cosmic ray instruments. The present study includes particles stopping in the last five analysed detectors of HIST, corresponding to an energy range of ~30 to ~180 MeV/nucleon for Ne, Mg and Si nuclei. Figure 14a shows mass histograms obtained in accelerator calibrations of HIST at the Bevalac by fragmenting an Fe beam in a polyethylene target, while Figure 14b shows flight data

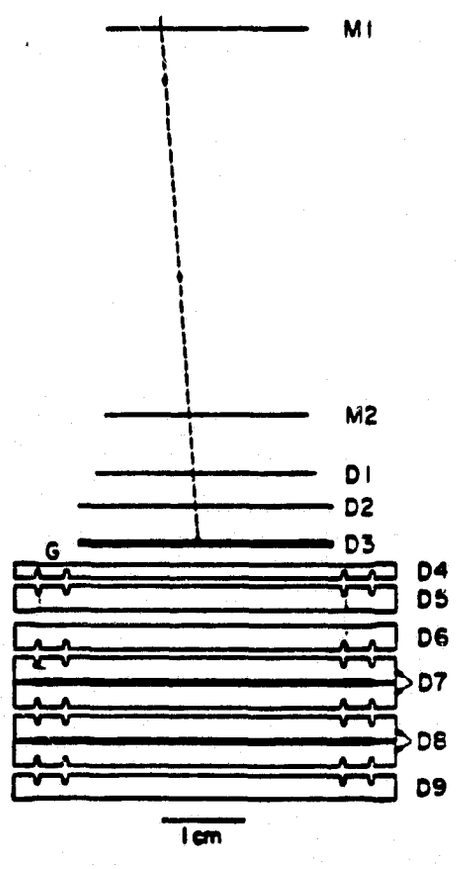

Figure 13

for the same energy range. Both data sets in Figure 14 have been analyzed in exactly the same manner, using identical selection criteria and instrument calibrations. The Bevalac data therefore provide absolute knowledge of the mass scale. The average mass resolution in the calibration data is $\sigma_m \approx 0.18$ amu, while in the flight data $\sigma_m \approx 0.20$ amu.

In Figure 15 we compare our observations with other reported measurements, and with the expected isotopic fractions (dotted line) for a cosmic ray source with solar system isotopic composition. Other investigations measured the mean mass of neon or the $^{22}Ne/^{20}Ne$ ratio, without determining the ^{21}Ne abundance. To include these measurements in Figure 15 we assumed a ^{21}Ne fraction of 0.11 at 1 AU, as is calculated assuming negligible ^{21}Ne at the source. Our observations are consistent with those earlier studies that find excess ^{22}Ne in the cosmic rays. In addition, our results suggest excesses of both ^{25}Mg and ^{26}Mg at the source.

In order to relate our observations at 1 AU to the cosmic ray source composition we performed interstellar propagation and solar modulation calculations. The source was assumed to have solar system isotopic composition with the exception of Ne, Mg, and Si, where the isotopic fractions were allowed to vary for comparison with the observations. We calculated the effect of solar modulation on the relative abundances of isotopes by evaluating numerical solutions of the Fokker-Planck equation. A convenient measure of the degree of solar modulation is the energy-loss parameter Φ where

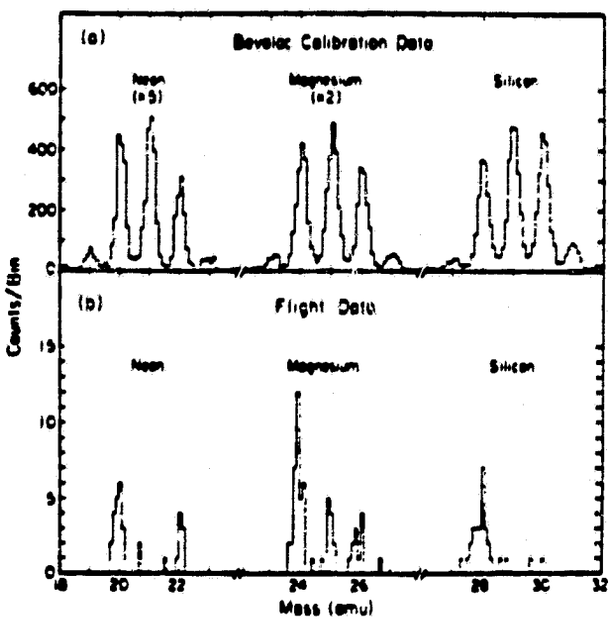

Figure 14

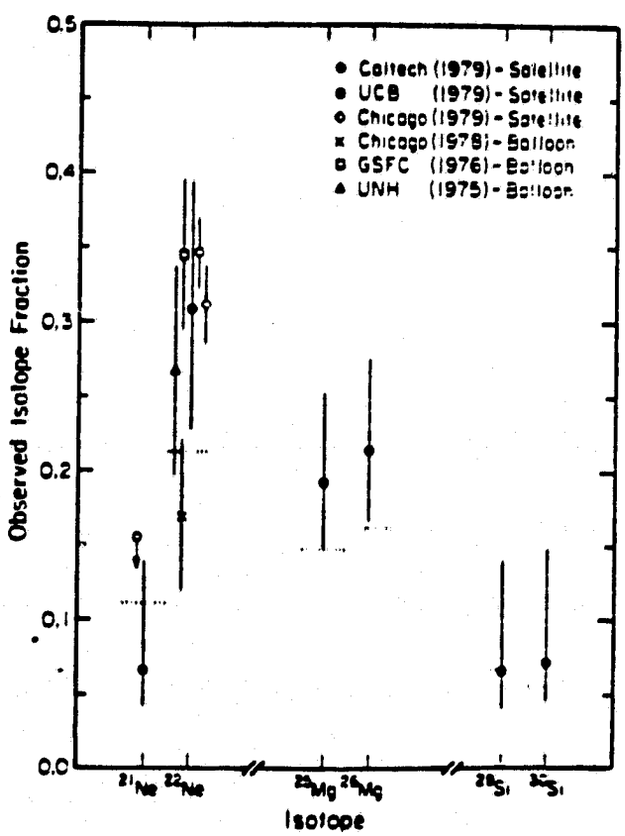

Figure 15

ϕ = 300 MeV/nucleon for 1978. Based on work by the Chicago group we used a source spectrum $dJ/dT = (T + E_0)^{-2.6}$, where T is the kinetic energy in MeV/nucleon and E_0 is a constant. Figure 16* shows the predicted $^{25}Mg + ^{26}Mg$ fraction at 1 AU as a function of the $^{25}Mg + ^{26}Mg$ fraction at the source for various combinations of ϕ and λ, assuming that ^{26}Al (half-life = 7×10^5 yr) decays. Also indicated are the 68% (1σ) and 90% (1.65σ) confidence intervals, as derived from the maximum likelihood analysis. Note that our observations imply a ($^{25}Mg + ^{26}Mg$) source fraction of $0.34^{+.09}_{-.07}$, significantly greater than the solar system fraction of 0.21. Using similar curves for the individual Ne, Mg and Si isotopes, we obtain the cosmic ray source composition in Table 1. The uncertainties in Table 1 include statistical uncertainties in the measurements, as well as uncertainties associated with propagation and modulation (which are typically ~ 0.01), as derived from the envelope of the calculated curves for $\lambda = (5.5 \pm 1)$ g/cm^2 and $\phi = (300 \pm 100)$ MeV/nucleon.

From Table 1 and Figure 15 we note that ^{22}Ne, ^{25}Mg and ^{26}Mg appear to be more abundant in the cosmic ray source than in the solar system. For the three satellite measurements shown in Figure 15, the mean observed ^{22}Ne fraction is 0.33 ± .02, corresponding to a cosmic ray source fraction of 0.27 ± .03, and a resulting $^{22}Ne/^{20}Ne$ source ratio ~ 3 times Cameron's solar system value of 0.12. For comparison, the ^{22}Ne fraction that we measure in solar flares is 0.12±.03 (see Status Report for 4/78 to 3/79) while the solar wind ^{22}Ne fraction is 0.07.

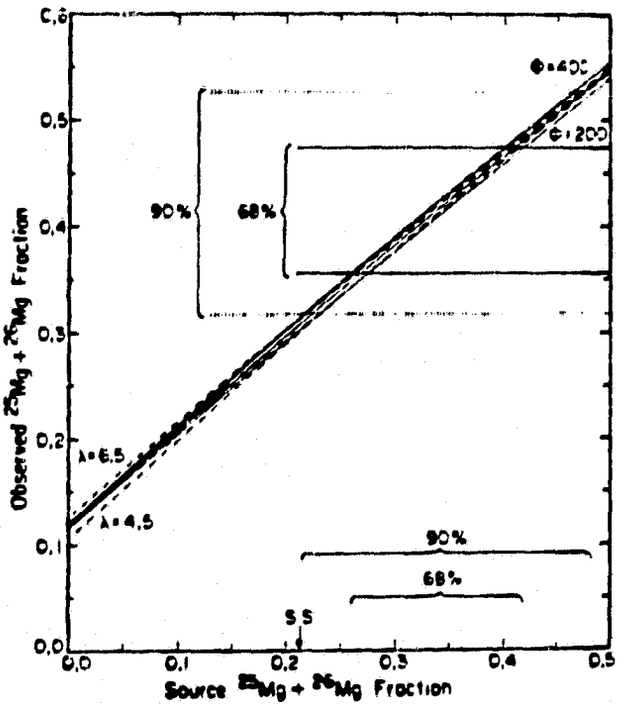

Figure 16

* The solid curves assume $\lambda = 5.5$ g/cm^2 and $\phi = 300 \pm 100$ MeV/nucleon. The dashed curves assume $\phi = 300$ MeV/nucleon and $\lambda = 4.5$ and 6.5 g/cm^2. Confidence intervals of 68% and 90% are indicated. The arrow marked S.S. indicates solar system fraction.

TABLE 1 - FRACTIONAL ISOTOPIC ABUNDANCES*

Isotope	Observed Fraction†	Cosmic Ray Source Fraction†	Solar System Fraction‡
^{20}Ne	$0.62^{+.06}_{-.11}$	$0.75^{+.13}_{-.14}$	0.889
^{21}Ne	$0.07^{+.07}_{-.03}$	< 0.06	0.003
^{22}Ne	$0.31^{+.08}_{-.08}$	$0.25^{+.14}_{-.13}$	0.108
^{24}Mg	$0.60^{+.04}_{-.07}$	$0.67^{+.07}_{-.09}$	0.787
^{25}Mg	$0.19^{+.06}_{-.04}$	$0.16^{+.07}_{-.06}$	0.101
^{26}Mg	$0.21^{+.06}_{-.04}$	$0.17^{+.08}_{-.06}$	0.112
$^{25}Mg + ^{26}Mg$	$0.40^{+.07}_{-.04}$	$0.33^{+.09}_{-.07}$	0.213
^{28}Si	$0.86^{+.03}_{-.11}$	$0.91^{+.03}_{-.12}$	0.922
^{29}Si	$0.07^{+.07}_{-.03}$	$0.04^{+.08}_{-.02}$	0.047
^{30}Si	$0.07^{+.08}_{-.03}$	$0.05^{+.07}_{-.03}$	0.031
$^{29}Si + ^{30}Si$	$0.14^{+.11}_{-.03}$	$0.09^{+.12}_{-.03}$	0.078

* The fraction relative to the total element abundance.

† 68% confidence intervals

‡ Cameron (1973)

For Mg, the derived (^{25}Mg + ^{26}Mg) source fraction of $0.33^{+.09}_{-.07}$ (Figure 16) corresponds to a (^{25}Mg + ^{26}Mg)/^{24}Mg source ratio that is $1.8^{+.08}_{-.05}$ times the solar system value of 0.27. From a maximum likelihood analysis we find both for ^{25}Mg/^{24}Mg and for ^{26}Mg/^{24}Mg, that there is less than a 10% probability that the cosmic ray source ratio is identical to that of the solar system. For (^{25}Mg + ^{26}Mg)/^{24}Mg the corresponding probability is only 5%. For ^{29}Si and ^{30}Si our observations are statistically limited, and the data do not rule out the possibility that these nuclei are also enhanced in the cosmic ray source.

Several mechanisms of nucleosynthesis are thought to contribute to Ne, Mg, and Si isotope production. The major contributions to solar system ^{20}Ne, ^{24,25,26}Mg and $^{29,\ 20}$Si are thought to come from explosive carbon burning, while $^{21,\ 22}$Ne production is the result of He burning, and ^{28}Si is due mainly to explosive oxygen burning. Woosley has suggested two factors that might lead to cosmic ray ^{22}Ne enhancements; we discuss below their implications for the Mg and Si isotopes.

One factor contributing to the ^{22}Ne enhancement might be continuing galactic evolution, since ^{22}Ne and other neutron-rich nuclei are second generation products of nucleosynthesis. Because the cosmic rays (age $\sim 2 \times 10^7$ years) are much younger than the solar system, they may reflect contributions from later stars of higher average metallicity. During helium burning, the larger abundance of metals will result in an increased abundance of ^{22}Ne which in turn is the source of an increased neutron excess η during explosive carbon burning. The Mg and Si isotopes are also sensitive to η. In recent calculations, Woosley and Weaver find that an initial stellar metallicity 2.5 times that of the solar system results in Ne, Mg, and Si isotopic abundances consistent with the cosmic ray source abundances presented here.

Since ^{20}Ne and ^{22}Ne are produced in different burning processes in different zones of a massive star, Woosley suggested that a second contributing factor to a non-solar ^{22}Ne/^{20}Ne ratio might be a variation in the relative contribution of these zones, as might be expected if the cosmic rays and the solar system come from stars of different average mass. Calculations by Couch, Schmiedekamp, and Arnett indicate that in stars with ~ 8 to $\sim 50\ M_\odot$, ^{22}Ne may provide a source of neutrons for a helium-burning s-process with significant yields of ^{25}Mg, ^{26}Mg, and other nuclei including, e.g., ^{58}Fe. A mixture of such helium-burning products with

typical carbon burning yields of ^{20}Ne and $^{24, 25, 26}Mg$ (and/or with additional material of solar system composition) could produce the cosmic ray source Ne and Mg composition (Table 1) if the helium-burning yield of $^{25}Mg + ^{26}Mg$ did not exceed that of ^{22}Ne, a constraint that places limits on the average mass of the stars involved. We conclude that an enrichment of helium burning products in cosmic rays can enhance both $^{22}Ne/^{20}Ne$ and $(^{25}Mg + ^{24}Mg)/^{24}Mg$, as observed, without significantly affecting ^{21}Ne or the silicon isotopes. Observations of other s-process nuclei in cosmic rays might test this possibility.

The Isotopic Composition of Galactic Cosmic Ray Iron Nuclei

Iron has long been recognized as one of the key elements for understanding the origin of galactic cosmic rays. Because ^{56}Fe has the largest binding energy/nucleon of the stable nuclei, it represents the end of the chain of nucleosynthetic products that can be formed by fusion reactions in stars. Theoretical studies show that the relative abundances of the iron isotopes are sensitive to the environment in which stellar nucleosynthesis occurs. Solar system Fe is more than 90% ^{56}Fe, but over a wide range of stellar environments ^{54}Fe is expected to be the dominant iron isotope, although compositions of intermediate character are also possible. Recent observations have now established that the $^{22}Ne/^{20}Ne$ ratio at the cosmic ray source is ~ 3 times that measured in high energy particles accelerated in solar flare events, suggesting that cosmic rays and solar system material may have different origins. If so, isotopic differences in Fe might also be expected.

Observations of the iron isotopes in cosmic rays have been limited by the experimental difficulties inherent in resolving adjacent isotopes that differ by only $\sim 2\%$ in mass. Although a number of earlier studies have suggested that the isotopic composition of cosmic ray iron may be characterized by non-solar abundances of ^{54}Fe and/or ^{58}Fe, there were also significant discrepancies between the various measurements. Recently studies using improved balloon-borne instrumentation concluded that cosmic ray iron is composed mainly of a single dominant isotope. Although the mass scale for these instruments was not calibrated in an absolute sense, supporting evidence was offered for a conclusion that ^{56}Fe is the dominant isotope, with only small amounts of ^{54}Fe and ^{58}Fe, as in the solar system

We have recently reported satellite observations of cosmic ray iron isotopes that directly establish that ^{56}Fe is the dominant cosmic ray Fe isotope. These observations cover an energy interval from 83 to 284 MeV/nucleon, with a mass resolution of σ_m = 0.37 amu. We obtain finite source abundances for ^{54}Fe and ^{56}Fe and upper limits on the source abundances of ^{55}Fe, ^{57}Fe, and ^{58}Fe, which, when compared to calculated nucleosynthesis yields, place significant constraints on the environment where cosmic ray Fe originates.

Figure 17a shows an Fe mass histogram obtained in accelerator calibrations of the flight HIST instrument with an ^{56}Fe beam at the Lawrence Berkeley Laboratory Bevalac (42,915 events). The Bevalac beam contained, in addition to ^{56}Fe, ~3% ^{54}Fe and other Fe isotopes produced in material used to reduce the beam energy. Figure 17b shows cosmic ray data from the same energy range (30 events). Comparisons of Bevalac and cosmic ray data for ^{20}Ne, ^{24}Mg, and ^{28}Si (see Figure 14) verify the instrument calibration was the same before and after launch. The Bevalac data, therefore, fix absolutely the mass scale. Both the calibration and the cosmic ray distributions are dominated by a well resolved peak at ^{56}Fe. There is also evidence for ^{54}Fe in the flight data, but no evidence for iron isotopes heavier than ^{56}Fe. The mass resolution in the calibration data is σ_m = 0.32 amu, while in the flight data, σ_m = 0.37 ± .05 amu for the ^{56}Fe peak. To our knowledge, this is the first cosmic ray Fe isotope measurement with a directly calibrated absolute mass scale.

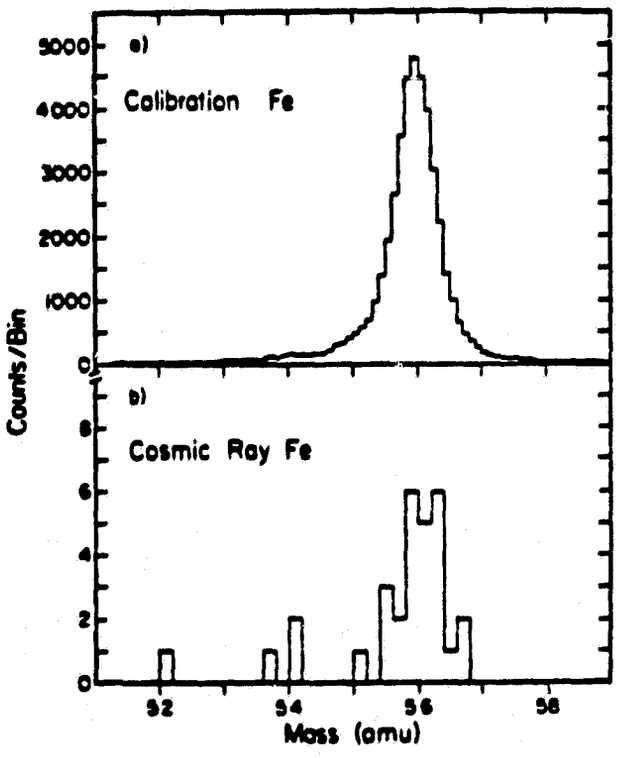

Figure 17

Table 2 summarizes the observed isotopic composition at 1 AU. In Figure 18 we compare* our observations with recent balloon measurements, and with expected isotopic distribution resulting from a solar system source. Within the quoted uncertainties, the measurements in Figure 18 are consistent with each other, and with the expected composition resulting from a cosmic ray source of solar system isotopic composition. They show no evidence for the large contributions of ^{58}Fe reported by some earlier experiments with apparently poorer resolution, or for large contributions of ^{54}Fe ($\geq 25\%$) that have been reported.

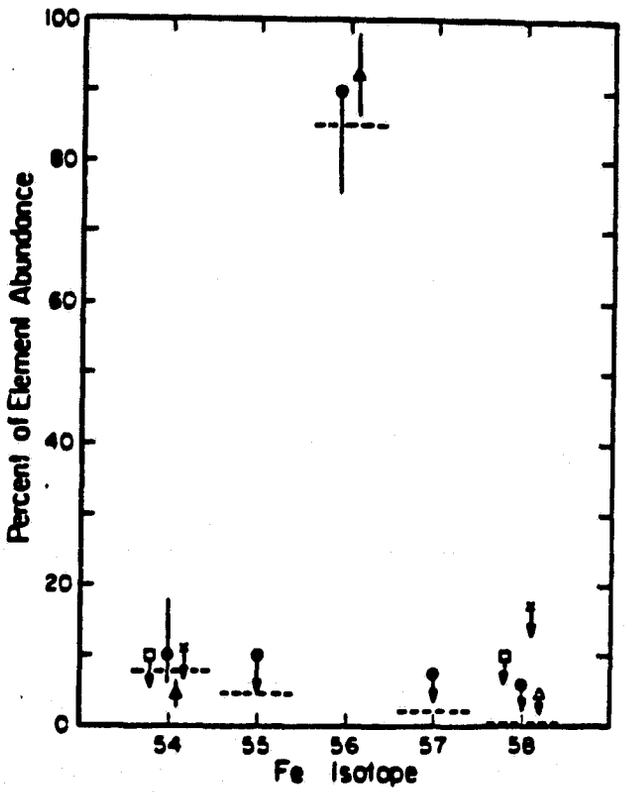

Figure 18

We have derived the cosmic ray source composition consistent with our observations by performing interstellar propagation and solar modulation calculations. Table 2 includes the source composition of iron isotopes that we derive with their 68% confidence intervals. Also shown in Table 2 is the solar system isotopic composition of Fe. We see no evidence for a cosmic ray source composition unlike that of the solar system, a conclusion also reached by the most recent studies using balloon-borne instrumentation. It is evident, however, that high resolution measurements with signicantly

---

* References for the measurements: solid circles (Caltech); squares (U.C. Berkeley, balloon); triangles (New Hampshire, balloon); crosses (Minnesota, balloon). The dotted lines show the calculated abundances at 1 AU for a solar system source composition, assuming that all ^{56}Fe produced during propagation survives.

TABLE 2 - Fe ISOTOPE COMPOSITION*

Isotope	Observed (%)+	Cosmic Ray+ Source (%)	Solar‡ System (%)
^{54}Fe	10^{+8}_{-4}	9^{+8}_{-5}	5.8
^{55}Fe	≤ 10	$\leq 7^{\S}$	0
^{56}Fe	90^{+0}_{-15}	91^{+5}_{-11}	91.7
^{57}Fe	≤ 8	≤ 8	2.2
^{58}Fe	≤ 6	≤ 6	0.3

* Percentage of total iron

+ 68% confidence intervals or 84% confidence limits

‡ Cameron (1973)

§ Assuming ^{55}Fe does not decay

better statistics will be needed for accurate determination of the ^{54}Fe, ^{57}Fe, and ^{58}Fe source abundances.

The nucleosynthesis of Fe is thought to take place in high-temperature, high-density regions of massive stars under conditions of nuclear-statistical equilibrium (e-process). The isotope distribution of the Fe-peak elements (Cr through Ni) that results is a sensitive function of the neutron excess $\eta = (n_n - n_p)/(n_n + n_p)$, where n_n and n_p are the neutron and proton densities of the stellar zone where nucleosynthesis occurs. Hainebach, Clayton, Arnett, and Woosley (HCAW) have concluded that the solar system iron-peak elements are made up of at least two components characterized by different values of η. In their 2-zone solution, a low-η component ($\eta = .004$) contributes $\sim 97\%$ of solar system Fe and includes ^{54}Fe, ^{56}Fe, and ^{57}Fe with relative abundances in agreement with the observed solar system composition. Under these conditions, ^{56}Fe and ^{57}Fe were actually synthesized as ^{56}Ni and ^{57}Ni. A smaller contribution ($\sim 3\%$) from a high-η zone ($\eta = .077$) is required to reproduce the observed ^{58}Fe abundance. It would be surprising if cosmic ray Fe consisted of exactly the same mixture of the same two components, since cosmic rays and solar system material might well originate in stars of different masses, and/or at different stages of the evolution of the galaxy.

Figure 19 shows calculated isotope mass fraction ratios* resulting from the e-process calculations of HCAW as a function of the neutron excess η. The $^{55}Mn/^{56}Fe$ curves assume that all ^{55}Fe produced in the source decays to ^{55}Mn by electron-capture (half-life = 2.6 yr.). Also shown are measurements of these ratios for the solar system, as tabulated by Cameron, and for cosmic rays. Note that the cosmic ray ratios for the Fe isotopes and for $^{55}Mn/^{56}Fe$ are consistent with either a "high-η" (~ 0.07) or a "low-η" (0.002-0.007) solution, neither of which reproduces the $^{60}Ni/^{58}Ni$ observations. The

---

* Isotope mass fraction ratios as a function of the neutron excess η The curves are from calculations by HCAW. The open triangles are the solar system abundances after Cameron. The cosmic ray Fe measurements (solid circles) are from Caltech only, while the $^{60}Ni/^{58}Ni$ point is based on measurements by Berkeley and Minnesota. We show also the conservative limits $^{52}Cr/^{56}Fe \leq 0.04$ and $^{55}Mn/^{56}Fe \leq 0.03$, based on the cosmic ray source elemental ratios $Cr/Fe \leq 0.03$ and $Mn/Fe \leq 0.02$. In the top panel, regions of η consistent with the cosmic ray observations are indicated.

$^{52}Cr/^{56}Fe$ observations require $\eta \leq 0.05$. The Berkeley group concluded from their Fe and Ni isotope observations that the cosmic rays required contributions from more than one e-process zone for production, much as HCAW concluded for the solar system. Alternatively, the cosmic ray source may represent a mixture of a single e-process zone and some other nucleosynthetic process which contributes, for example, to the ^{60}Ni abundance.

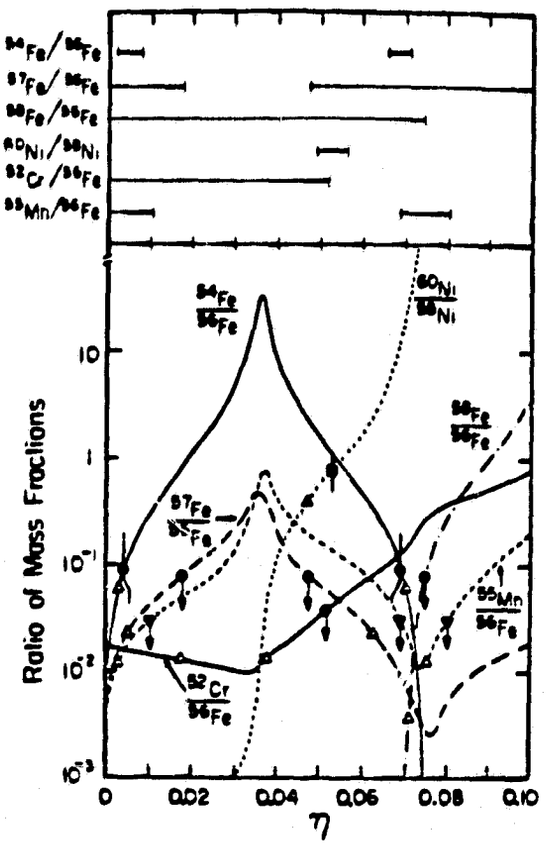

Figure 19

In either case, it is of interest to determine the maximum contribution a given e-process zone can make to the cosmic ray source material. From a comparison of the measured and calculated isotopic ratios, such as those in Figure 19, we have computed the maximum allowed percentage of cosmic ray ^{56}Fe that can derive from a zone with a particular value of η. We reasoned that if a given zone produces more of a specific isotope relative to ^{56}Fe than is observed, then that zone can make only a limited contribution to the total production of ^{56}Fe. For example, note in Figure 19 that the e-process calculations give $^{58}Fe/^{56}Fe = 1$ at $\eta = 0.09$, while the cosmic ray upper limit is $^{58}Fe/^{56}Fe \leq 0.08$. It follows that no more than 8% of the ^{56}Fe can derive from this e-process zone. In general, only for zones with $\eta \leq 0.01$ can the contribution to ^{56}Fe be $\geq 50\%$ and still satisfy all isotopic constraints. Hainebach et al. (1974) have reached similar conclusions in treating the synthesis of the solar system iron-peak nuclei. Note, however, that the range $\eta \leq 0.01$ still allows for significant differences in the cosmic ray and solar system isotope distribution.

For example, the evidence for enhanced abundances of the neutron-rich isotopes of Ne and possibly Mg in cosmic rays may be interpreted as due to an η (or metallicity) value somewhat greater than characterizes solar system material, possibly due to galactic evolution effects. This might suggest an

e-process η value of ≥ 0.004, not incompatible with the present cosmic ray Fe isotope observations. Further observations should establish whether the neutron-rich character of cosmic ray Ne extends to heavier elements, including Fe, thereby providing possible evidence for on-going nucleosynthesis in the galaxy.

4. A Heavy Nuclei Experiment (HNE) launched on HEAO-3 in September, 1979

The Heavy Nuclei Experiment (HNE) is a joint investigation involving this group and M.H. Israel, J. Klarmann (Washington University), W.R. Binns (McDonnell-Douglas), and C.J. Waddington (University of Minnesota). HNE is designed to measure the elemental abundances of relativistic high-Z cosmic ray nuclei ($17 \leq Z \leq 130$). The results of such measurements are of significance to the studies of nucleosynthesis and stellar structures, the existence of extreme transuranic nuclei, the origin of cosmic rays, and the physical properties of the interstellar medium.

HNE was successfully launched on HEAO-3 in September, 1979 and continues to function well after 6 months in orbit. Ultraheavy nuclei are being observed at the rate of $\sim$ 15/day. With detailed analysis of $\sim$ 70 days of data, distinct peaks have been observed for $_{28}$Ni and $_{30}$Zn and there is evidence for abundance peaks for even-Z elements up thru Z=38. The first series of presentations are currently in preparation for the Spring Meeting of the American Physical Society.

5. A Comprehensive Particle Analysis System (COMPAS) for the Solar Polar Mission

This investigation was proposed jointly by this group and by J.H. Trainor, M.A.I. Van Hollebeke, and T.T. von Rosenvinge (GSFC), G. Gloeckler and G.M. Mason (U of Md.), D. Hovestadt and B. Klecker (MPI, Munich, FRG), and L.A. Fisk and W.R. Webber (UNH). COMPAS is designed to measure the energy spectra, elemental composition, and streaming patterns of energetic nuclei from H through Fe from energies of about 40 keV/nuc to about 400 MeV/nuc. Isotope resolution is provided for H and He in the 0.10 to 64 MeV/nuc energy range up through Fe in the 13 to 400 MeV/nuc range. Electron spectra and their angular distributions will be measured between 30 keV and 120 MeV. COMPAS will use the unique Solar Polar trajectory opportunity to observe energetic particle phenomena at essentially all

solar latitudes in the heliosphere. The study of galactic cosmic rays at high latitudes will emphasize the spectral differences and streaming patterns of elements, isotopes, and electrons that have low energies in the interstellar medium and are not observable in the ecliptic. Other studies will provide information on small flares and coronal propagation of energetic particles at higher latitudes, on the latitude-dependent interplanetary acceleration mechanisms, on the origin of the anomalous low-energy cosmic ray component, on the heliospheric propagation of electrons, and on the origin, acceleration, and behavior of energetic particles in the outer Jovian magnetosphere.

The Caltech group is responsible for the overall management of COMPAS and for the detailed design of the Mass Spectrometer Telescope (MAST) and the Proton/Electron Telescope (PET). The detailed design of MAST and PET is essentially complete and breadboards of the precision analog circuits have been tested. The Preliminary Design Review for COMPAS was held March 31, 1980.

6. A Solar and Galactic Experiment (SAGE) Proposed for the IPL Spacecraft of the OPEN Program

This investigation was proposed jointly by this group and by M. Garcia-Munoz, J.A. Simpson, and J.P. Wefel of the University of Chicago. SAGE is designed to provide measurements of the isotopic composition of solar and galactic cosmic rays with a collection factor ten times that of COMPAS for nuclei from $_{1}H$ through $_{40}Zr$ with energies ranging from $\lesssim$ 5 MeV/nuc to $\gtrsim$ 500 MeV/nuc. The large collection factor will make possible the statistical precision necessary for the study of the important but rare nuclides such as the neutron-rich species ^{35}S, $^{46,48}Ca$, ^{58}Fe, and $^{62,64}Ni$ and acceleration delay-time clocks such as ^{57}Co and ^{59}Ni. These studies will concentrate on an accurate comparison of the isotopic composition of galactic cosmic ray source material with that of the Sun as a means of investigating the nature of the nucleosynthesis processes occurring in the Galaxy. Other studies will address acceleration and propagation processes both in the Solar System and in the Galaxy.

B. ACTIVITIES IN SUPPORT OF OR IN PREPARATION OF SPACECRAFT EXPERIMENTS

These activities generally embrace prototypes of experiments on existing or future NASA spacecraft or they complement and/or support such observations.

1. The High Energy Isotope Spectrometer Telescope (HEIST)

HEIST is a balloon-borne detector system designed to provide high resolution isotopic measurements for cosmic ray nuclei with $3 \leq Z \leq 28$ in the energy interval $60 \leq E \leq 700$ MeV/nucleon, complementing the measurements with this group is making with the HIST instrument on ISEE-3.

The doctoral dissertation based on HEIST data is nearing completion. Accurate maps of the CsI scintillators have been obtained and the calibration of the position-sensing multi-wire proportional counters has been refined. Mass histograms for carbon have been obtained using the multiparameter mass-measurement technique developed for the analysis of HIST isotope data.

2. Antiproton and Antihelium Balloon Experiment

The antimatter ($\bar{p}$) experiment (which became an SRL project with Dr. A. Buffington's move from Berkeley to Caltech in Fall 1979) is ready for a balloon campaign in Canada this summer. A number of improvements have been made in the optics and electronics; except for these the payload will be flown as it had been prepared for flight last summer. The launch site has been moved from Thompson, Manitoba, to The Pas, Manitoba, to take advantage of the latter site's improved runways and reduced air traffic. This change may cut into the flight data statistics and/or introduce systematic errors, because the geomagnetic cutoff for the flight will be somewhat increased. The antiprotons lost due to this effect could be as much as 25% of the total, or may be none at all; accurate cutoff measurements are lacking at these geomagnetic latitudes. Thus the changed launch site represents a potential compromise between optimum launch/recovery conditions, geographic accessibility, and geomagnetic distortion of the data-taking. To improve the chances of a successful launch, a larger balloon has been procured which permits carrying sunset ballast. This should widen the allowed launch window to nearly a full 24 hours per day.

A measurement of cosmic-ray antiprotons has recently been reported [R.L. Golden et al., Phys. Rev. Lett. 43, 1196 (October, 1979)], with a $\bar{p}/p$ ratio of 5×10^{-4}. If this ratio also holds at the tenfold reduced incident energy covered by this experiment, over 2000 $\bar{p}$'s should be recorded in a nominal flight goal of ten hours live time for the apparatus. This would represent a nearly one hundred-fold increase in event statistics over the recently reported measurement, and with no calculated background event

subtraction being required. In fact, the $\bar{p}/p$ ratio is expected to be much smaller at our low energies, due to kinematical effects in the production of $\bar{p}$'s in interstellar space, if our measurement were to take place outside of the solar cavity. The adiabatic deceleration of cosmic rays within the solar cavity should, however, cause our experiment to be measuring $\bar{p}$'s that came from a significantly higher energy away from the sun than what we observe for them here. Thus this experiment will hopefully both confirm the previous $\bar{p}$ measurement and provide a significant new direct measurement of the adiabatic deceleration.

3. γ-Ray Spectroscopy

Gamma ray astronomy was initiated as a new research activity of the SRL group during the summer of 1979 with Dr. T. Prince accepting lead responsibility. To date activity has centered on developing a strong collaborative research effort with the high energy astrophysics group at Caltech's Jet Propulsion Laboratory, headed by Dr. A.S. Jacobson. Projects have been undertaken in a number of different areas of mutual interest including data analysis and gamma ray detector technology development. Data analysis work is currently proceeding on HEAO C-1 data, with the specific purpose of investigating gamma ray burst phenomena, and also on data from the JPL group's balloon-borne gamma ray spectrometer which observed the Cygnus region in May of 1978. The technology development has focused on identifying promising new approaches to high resolution gamma ray spectroscopy. Special attention has been given to the prospects of developing position sensitive solid-state detectors for use in a solid state, high resolution Compton telescope and also to the prospects of utilization of Mercuric Iodide (HgI_2) as a high-Z, room temperature solid-state detector. In addition to these activities, work has recently begun on the design of a next-generation balloon-borne gamma ray spectrometer, the fabrication of which will be a joint SRL-JPL project.

4. Thermal-Vacuum Test Facilities

The thermal-vacuum solid state detector (SSD) test facilities at the SRL have recently been updated, reflecting state of the art improvements in vacuum technology. In particular, older type oil-diffusion pumps have been replaced with modern cryopumps, permitting rapid achievement of high and ultra-high vacuum conditions, with no possibility of test chamber

contamination due to pump oil migration through backstreaming or system malfunction. The addition of surface area and molecular sieve traps in a series mode between the cryopumps and the mechanical roughing pumps, eliminates the possibility of oil backstreaming from the latter source. In addition, the use of cryopumps eliminates the previous LN_2 requirements, resulting in simplified system operation and a reduction in operating costs.

The vacuum test facilities consist basically of three specialized pumping stations. For discussion purposes, these are designated the A, B, and Thermal Vacuum Station (TVS).

The A and B stations have been fitted with identical CTI Cryotorr-7 cryopumps, utilizing a single air-cooled helium compressor for economy. The compressor has the capacity to operate both cryopumps simultaneously, or each station individually, with no loss in pumping efficiency. Both stations normally operate at room ambient temperature, with demonstrated capability for continuous pumping at $1X10^{-6}$ torr. Full vacuum capacity is achieved in approximately one hour from a "warm" (room temperature) startup. Once full vacuum conditions are achieved in the cryopump, each system is capable of repeated cycling of the vacuum test chamber from atmospheric pressure to full vacuum with a nominal duty cycle of 15 minutes. Both stations are fitted with electrical feedthroughs and remote positioning devices for vacuum testing applications.

The TVS provides accurate thermal control of its test environment in addition to ultra-high vacuum capability. The station has been fitted with a Perkin-Elmer Series 4 cryopump, employing a water- cooled helium compressor. To date, the system has demonstrated the capacity for continuous vacuum pumping at a level of approximately 7×10^{-8} torr, with the vacuum test chamber at a nominal temperature of $+20^{\circ}C$. Additional thermal testing is planned to establish the cryopump response characteristics over the anticipated thermal operating range of the test chamber, namely $-40^{\circ}C$ to $+40^{\circ}C$.

Due to operating differences between the cryopumps and oil-diffusion pump, the system controller required redesign and construction. Various interlocks were also incorporated into the design, reducing the possibility of operator error either damaging the vacuum system, or subjecting the components under test to conditions outside the specified test range. This phase of construction and testing has been completed, with the new

controller electronics having met all design requirements.

A new data recording system has been added to the thermal-vacuum SSD facility, replacing the existing analog chart recorders. This consists of two Datel digital printers, incorporating a variable operator-selected data print cycle over the range of 30 seconds to 2 hours. The digital printers are used in association with a Kennedy incremental magnetic tape recorder, providing a data record with a 10 second recording cycle, suitable for more detailed data analysis. The digital printers provide on-line access to various thermal-vacuum parameters, as well as selected output parameters of the components under test.

The data recording system described above is currently undergoing reliability testing and calibration.

C. OTHER ACTIVITIES

E.C. Stone has continued serving as NASA's Project Scientist for the Voyager Missions. He is also a member of the Committee on Space Astronomy and Astrophysics of the Space Science Board and has almost completed his term as chairman of the Cosmic Physics Division of the American Physical Society. He continues to serve on the High Energy Astrophysics Management Operations Working Group.

II Theory of Particles and Fields in Space

As a member of the Pioneer Saturn Vector Helium Magnetometer team whose Principal Investigator is E.J. Smith of JPL, L. Davis directed the analysis of the models of Saturn's magnetic field based on data taken within 10 Saturn radii of its center during the September encounter. The main results obtained thus far are that Saturn's field in this region is generally like that of earth scaled to Saturn's size but with a number of significant differences.

From the models we see that the magnetic field is predominantly dipolar as are the fields of the earth and Jupiter but with relatively smaller asymmetries and non-dipolar components. The field near Saturn's magnetic equator is close to 0.20 gauss as compared to 0.3 gauss for the earth and 4 gauss for Jupiter. This is less by a factor of 3 to 5 than the values expected from conjectured scaling laws and from the uncertain early reports of decametric bursts from the neighborhood of Saturn. An important and unexpected aspect of Saturn's field is its near axial symmetry. The tilt of Saturn's dipole from its rotation axis is of the order of 1^{o} whereas those

for the earth and Jupiter are of the order of 10^0. The displacement of the best fit dipole from the geometric center of the planet ranges from 1 to 5 percent of the radius, depending on just how the fit is made, whereas the corresponding displacements for the earth and Jupiter are substantially larger. In the spherical harmonic analysis for Saturn, the ratio of the higher order terms to the axial dipole term is smaller than it is for the other two planets.

All this suggests that Saturn's dynamic core is relatively smaller than those for the earth and Jupiter. This has indeed been predicted by some of the models of Saturn's interior. The greater symmetry strongly indicates that planetary dynamics do not require the degree of asymmetry observed for the earth and Jupiter and suggested as necessary by some, but not all, of the theorists working on dynamo theory. The greater simplicity of the Saturnian source should greatly reduce and perhaps eliminate some of the complications of the earth's and Jupiter's magnetospheres and provide us with a less complicated model to study and try to understand.

The exterior source terms, presumably produced by currents in the magnetopause or distributed more generally in the magnetosphere are of the order of 10 to 15 nT (10^{-5} gauss = 1 nanotesla = 1 gamma) depending on whether data inside 5 R_s, or that inside 8 R_s, are used. This suggests that the magnetopause currents may be contributing roughly 40% to 80% of the field ascribed by the spherical harmonic analysis to sources external to 5 to 8 R_s from the center. This would be consistent with the fields observed just inside the magnetopause. The remainder might be produced by currents, perhaps current sheets, deep in the magnetosphere. Alternatively, the remainder could be an artifact resulting from the biased distribution in position of the trajectory along which the data for the spherical harmonic analysis had to be taken.

III. BIBLIOGRAPHY

1978

Althouse, W.E., A.C. Cummings, T.L. Garrard, R.A. Mewaldt, E.C. Stone, and R.E. Vogt, "A Cosmic Ray Isotope Spectrometer", IEEE Transactions on Geoscience Electronics, GE-16, 204, (1978).

Baker, D.N., and E.C. Stone, "The Magnetopause Energetic Electron Layer 1, Observations Along the Distant Magnetotail", J. Geophys. Res., 83, 4327, (1978).

Baker, D.N., E. W. Hones, and E.C. Stone, "Fast Electrons Near the Magnetopause and Their Dependence on Interplanetary Parameters", EOS Trans. AGU 59, 365, (1978).

Conlon, T.F., N. Lal, F.B. McDonald, J.H. Trainor, E.C. Stone, and R.E. Vogt, "Observations of Solar Cosmic Ray Events by the Voyager 1 & 2 Cosmic Ray Experiment", Bull. Am. Phys. Soc. 23, 508, (1978).

Cook, W.R., E.C. Stone, R.E. Vogt, F.B. McDonald, and J.H. Trainor, "The Elemental Composition of Low Energy Cosmic Ray Nuclei During Recurrent Events", Ibid, 23, 509, (1978).

Cook, W.R., E.C. Stone, R.E. Vogt, T.F. Conlon, and W.R. Webber, "Elemental Composition ($1 \leq Z \leq 26$) of Solar Energetic Parcicles Sept. 1977 - April 1978", EOS Trans. AGU 59, 1151, (1978).

Cummings, A.C., T.L. Garrard, E.C. Stone, R.E. Vogt, and J.R. Jokipii, "The Streaming of Low Energy Protons Observed Between 1 and $\sim$ 2.5 AU", Bull. Am. Phys. Soc. 23, 509, (1978).

Cummings, A.C., T.L. Garrard, E.C. Stone, and R.E. Vogt, "Characteristics of Recurrent Energetic Particle Events Observed Between 1 and $\sim$ 4 AU", EOS Trans. AGU 59, 1153, (1978).

Davis, L. Jr., E.J. Smith, B.T. Tsurutani, and J.H. Wolfe, "Properties of the Interplanetary Current Sheet," Ibid, 59, 365, (1978).

Garrard, T.L., A.C. Cummings, E.C. Stone, R.E. Vogt, J.H. Trainor, and J.R. Jokipii, "A Comparison of Diffusive Proton Streaming With Magnetic Field Direction", Ibid 59, 1153, (1978).

Hartman, S.H., E.C. Stone, and R.E. Vogt, "Jovian Electron Increases at 1 AU and the Large Scale Structure of the Interplanetary Medium", Ibid, 59, 1173, (1978).

1978

Lin, R.P., R.A. Mewaldt, E.C. Stone, R.E. Vogt, C. Paizis, and M.A.I. Van Hollebeke, "Spectral and Temporal Characteristics of Solar Electrons from 20 keV to 20 MeV", Bull. Am. Phys. Soc. 23, 509, (1978).

Marshall, F.E., and E.C. Stone, "Characteristics of Sunward Flowing Proton and Alpha Particle Fluxes of Moderate Intensity", J. Geophys. Res., 83, 3289, (1978).

Mewaldt, R.A., E.C. Stone, and R.E. Vogt, "Spectral Characteristics of Recurrent Proton and Alpha Particle Streams at 1 AU", Bull Am. Phys. Soc. 23, 509, (1978).

Mewaldt, R.A., E.C. Stone, and R.E. Vogt, "The Radial Diffusion Coefficient of 1.3 - 2.3 MeV Protons in Recurrent Proton Streams", Geophys. Res. Ltrs. 5, 965, (1978).

Mewaldt, R.A., J.D. Spalding, E.C. Stone, and R.E. Vogt, "First Results From the Heavy Isotope Spectrometer Telescope on ISEE-C", EOS Trans. AGU 59, 1152, (1978).

Stone, E.C., "The Streaming of 1.8 to 8 MeV Protons During Recurrent Events Observed Between 1 and ~ 2.5 AU", Ibid, 59, 332, (1978).

Stone, E.C. "An Introduction to the Voyager Mission", Ibid, 59, 331, (1978).

Stone, E.C., and M.E. Wiedenbeck, "The Derivation of the Cosmic Ray Source Abundances from Observed Isotopic Composition", Bull. Am. Phys. Soc. 23, 619, (1978).

Stone, E.C., R.A. Mewaldt, and R.E. Vogt, "The Radial Diffusion of Coefficient of 1.3-2.3 MeV Protons During Recurrent Proton Streams", Ibid, 23, 509, (1978).

Stone, E.C., "An Overview of the Voyager Mission to the Outer Solar System", Ibid, 23, 536, (1978).

Stone, E.C., "Voyager Investigations of the Saturnian System", The Saturn System, NASA Conference Publication 2068, 285, (1978).

Trainor, J.H., F.B. McDonald, T.F. Conlon, W.R. Webber, E.C. Stone, and R.E. Vogt, "Studies of the Composition of Solar Cosmic Rays by Voyager 1 & 2 Cosmic Ray Experiment", Bull. Am. Phys. Soc. 23, 508, (1978).

1979

Bieber, J.W., and E.C. Stone, "Energetic Electron Bursts in the Magnetopause Electron Layer and Interplanetary Space", EOS Trans. AGU 60, 369, (1979).

Bieber, J.W., and E.C. Stone, "Energetic Electron Bursts in the Magnetopause Electron Layer and in Interplanetary Space", Proceedings of Magnetospheric Boundary Layers Conference, Alpbach, Austria, ESA SP-148, 131, (1979).

Bieber, J.W., and E.C. Stone, "Simultaneous Two-Spacecraft Observations of the Magnetopause Electron Layer", EOS Trans. AGU 60, 909, (1979).

Conlon, T.F., F.B. McDonald, A.W. Schardt, J.H. Trainor, E.C. Stone, and R.E. Vogt, "Source Variations of Interplanetary Jovian Electrons: Voyagers 1 and 2", EOS Trans. AGU 60, 354, (1979).

Conlon, T.F., F.B. McDonald, M.A.I. Van Hollebeke, J.H. Trainor, W.R. Webber, E.C. Stone, and R.E. Vogt, "The Effect of Coronal Transport on Energetic Solar Particles", Bull. Am. Phys. Soc. 24, 659, (1979).

Conlon, T.F., A.W. Schardt, F.B. McDonald, J.H. Trainor, and N. Gehrels, "The Detection of Interplanetary Protons Deep in Jupiter's Magnetosphere", EOS Trans. AGU 60, 919, (1979).

Cook, W.R., E.C. Stone, R.E. Vogt, J.H. Trainor, and W.R. Webber, "Elemental Composition of Solar Energetic Particles in 1977 and 1978". 16th International Cosmic Ray Conference, Kyoto, Japan, Conf. Papers 12, 265, (1979).

Gehrels, N.C., E.C. Stone, R.E. Vogt, and J.H. Trainor, "Energetic Sulfur and Oxygen Nuclei in the Jovian Magnetosphere", EOS Trans. AGU 60, 919, (1979).

Hartman, S.H., "Observations of 1 - 6 MeV Jovian Electrons at 1 AU and a Study of Their Propagation", Ph.D. Thesis, California Institute of Technology, (1979).

Lal, N., F.B. McDonald, T. Conlon, J.H. Trainor, W.R. Webber, E.C. Stone, and R.E. Vogt, "The Modulation and Radial Variation of the Anomalous Helium and Oxygen Component Observed by Voyagers 1 and 2", Bull. Am. Phys. Soc. 24, 564, (1979).

1979

McDonald, F.B., J.H. Trainor, N. Lal, E.C. Stone, R.E. Vogt, and W.R. Webber, "The Charge and Energy Spectra of Low Energy Galactic Cosmic Rays", Ibid, 24, 564, (1979).

Mewaldt, R.A., "Isotopic Measurements of Solar and Galactic Cosmic Rays", EOS Trans. AGU 60, 907, (1979).

Mewaldt, R.A., "Studies of Elemental and Isotopic Composition of Solar Flare Nuclei", Bull. Am. Phys. Soc. 24, 618, (1979).

Mewaldt, R.A., J.D. Spalding, E.C. Stone, and R.E. Vogt, "The Isotopic Composition of Solar Flare Accelerated Neon", Ap. J. 231, L97, (1979).

Mewaldt, R.A., J.D. Spalding, E.C. Stone, and R.E. Vogt, "Satellite Measurements of the Isotopic Composition of Galactic Cosmic Rays", 16th International Cosmic Ray Conference, Kyoto, Japan, Conf. Papers 12, 86, (1979).

Mewaldt, R.A., J.D. Spalding, E.C. Stone, and R.E. Vogt, "Isotopic Measurements of Energetic Heavy Nuclei in the Solar Flares", Bull. Am. Phys. Soc. 24, 694, (1979).

Mewaldt, R.A., J.D. Spalding, E.C. Stone, and R.E. Vogt, "The Isotopic Composition of Energetic Solar Flare Nuclei from Carbon Through Iron", 16th International Cosmic Ray Conference, Kyoto, Japan, Conf. Papers 5, 74, (1979).

Mewaldt, R.A., E.C. Stone, and R.E. Vogt, "Characteristics of the Spectra of Protons and Alpha Particles in Recurrent Events at 1 AU", Geophys. Res. Ltrs. 6, 589, (1979).

Smith, E.J., L. Davis, Jr., D.E. Jones, P.J. Coleman, Jr., P. Dyal, and C.P. Sonnet, "Saturn's Magnetic Field and Magnetosphere: Pioneer 11", EOS Trans. AGU 60, 865, (1979).

Smith, E.J., D.E. Jones, B.T. Tsurutani, and L. Davis, Jr., "Magnetic Detection of the Satellite 1979 S-1 (Saturn) by Pioneer 11", Ibid, 60, 866, (1979).

Spalding, J.D., R.A. Mewaldt, E.C. Stone, and R.E. Vogt, "Satellite Measurements of the Isotopic Composition of Galactic Cosmic Rays", Bull. Am. Phys. Soc. 24, 692, (1979).

1979

Spalding, J.D., R.A. Mewaldt, E.C. Stone, and R.E. Vogt, "The Isotopic Composition of Heavy Nuclei Accelerated in Solar Flares", EOS Trans. AGU 60, 907, (1979).

Stilwell, D.E., W.D. Davis, R.M. Joyce, R.B. McDonald, J.H. Trainor, W.E. Althouse, A.C. Cummings, T.L. Garrard, E.C. Stone, and R.E. Vogt, "The Voyager Cosmic Ray Experiment", IEEE Trans. on Nuclear Science, NS-26, 513, (1979).

Stone, E.C., "An Overview of the Voyager 1 Encounter with Jupiter", EOS Trans. AGU 60, 304, (1979).

Stone, E.C., "Streaming Anisotropies of 1.3 - 2.3 MeV Protons and Their Interpretation", Ibid, 60, 739, (1979).

Stone, E.C., W.R. Cook, R.E. Vogt, W.R. Webber, F.B. McDonald, J.H. Trainor, and N. Lal, "The Elemental Composition and Anisotropies of Low Energy Cosmic Rays Using Voyager Data", Bull. Am. Phys. Soc. 24, 564,(1979).

Stone, E.C., and A.L. Lane, "The Voyager 1 Encounter with the Jovian System", Science 204, 945, (1979).

Stone, E.C., and A.L. Lane, "Voyager 2 Encounter with the Jovian System", Science 206, 925, (1979).

Stone, E.C., and M.E. Wiedenbeck, "A Secondary Tracer Approach to the Derivation of Galactic Cosmic-Ray Source Isotopic Abundances", Ap. J. 231, 606, (1979).

Vogt, R.E., T.F. Conlon, W.R. Cook, A.C. Cummings, T.L. Garrard, N. Gehrels, J.R. Jokipii, N. Lal, F.B. McDonald, A.W. Schardt, E.C. Stone, J.H. Trainor, and W.R. Webber, "High Energy Particles", EOS Trans. AGU 60, 305, (1979).

Vogt, R.E., W.R. Cook, A.C. Cummings, T.L. Garrard, N. Gehrels, E.C. Stone, J.H. Trainor, A.W. Schardt, T. Conlon, N. Lal, and F.B. McDonald, "Voyager 1: Energetic Ions and Electrons in the Jovian Magnetosphere", Science 204, 1003, (1979).

Vogt, R.E., A.C. Cummings, T.L. Garrard, N. Gehrels, E.C. Stone, J.H. Trainor, A.W. Schardt, T.F. Conlon, and F.B. McDonald, "Voyager 2: Energetic Ions and Electrons in the Jovian Magnetosphere", Science 206, 984, (1979).

1980

Cook, W.R., E.C. Stone, and R.E. Vogt, "Elemental Composition of Solar Energetic Nuclei", accepted for publication in Ap. J. Letters (1980).

Mewaldt, R.A., "Spacecraft Measurements of the Elemental and Isotopic Composition of Solar Energetic Particles", to be published in Proceedings of the Conference on the Ancient Sun, Lunar & Planetary Science Institute, Houston (1980).

Mewaldt, R.A., J.D. Spalding, E.C. Stone, and R.E. Vogt, "High-Resolution Measurements of Galactic Cosmic-Ray Neon, Magnesium and Silicon Isotopes", Ap. J. Letters 235, L95 (1980).

Mewaldt, R.A., J.D. Spalding, E.C. Stone, and R.E. Vogt, "The Isotopic Composition of Galactic Cosmic Ray Iron Nuclei", accepted for publication in Ap. J. Letters (1980).

Smith, E.J., L. Davis, Jr., D.E. Jones, P.J. Coleman, Jr., D.S. Colburn, P. Dyal, and C.P. Sonett, "Saturn's Magnetic Field and Magnetosphere", Science 207, 407 (1980).